Rijksuniversiteit Groningen

university of groningen

faculty of science and engineering

Faculty of Science and Engineering

Discrete Technology & Production Automation

Power Sharing in DC Microgrids

Master thesis

Author:
V.J. (Vincent) Otten

Supervisors:
prof. dr. ir. J.M.A. Scherpen

prof. dr. C. De Persis

M. Cucuzzella, PhD

May 25, 2020

Abstract

A microgrid is an example of a distributed power system. Microgrids are defined as low-voltage distribution networks which comprise of various small-scale distributed generation units (DGUs), energy storage devices, and controllable loads that are connected through power lines. A microgrid must be controlled in such a way that it presents reliability and proper operation. One of the main challenges to assure reliability and proper operation of microgrids is the complex controllability of such a system.

In this research, a distributed control scheme is proposed that achieves fair power sharing and weighted average voltage regulation in dynamical DC microgrids. A microgrid is considered where DGUs are connected through dynamic resistive-inductive power lines and supply so-called ZIP-loads. Furthermore, every distributed generation unit is complemented with a local controller that communicates with neighboring controllers over a communication network. Achieving fair power sharing and weighted average voltage regulation reduces maintenance cost and prevents DGUs for breakdown which increases the stability and reliability of a power system.
The performance of the proposed distributed control scheme is investigated via extensive simulations. Many critical scenarios are simulated, including various network topologies, failure of power and communication lines and plug-and-play of DGUs. The simulation results show promising performance of the control scheme. Fair power sharing and average voltage regulation are achieved in most of the scenarios. Besides, the results lead to interesting insights regarding the design of microgrids. Theoretical validation of the control scheme is not included in this thesis and left for further research.

Contents

List of Figures

List of Tables

List of Acronyms

AC	Alternating Current
DC	Direct Current
DERs	Distributed Energy Resources
DGUs	Distributed generation units
GCOP	Grid connected operating mode
IOM	Islanded operating mode
LQR	Linear quadratic regulator
MG	Microgrid
MGCC	Main grid central controller
PCC	Point of common coupling
PID	Proportional integral derivative
PnP	Plug-and-play
PV	Photovoltaic
RES	Renewable energy source
SPOF	Single point of failure

List of Symbols

Calligraphic letters

$\mathcal{A}$	Adjacency matrix
$\mathcal{B}$	Incidence matrix
$\mathcal{D}$	Degree matrix
$\mathcal{E}$	Set of edges
$\mathcal{E}^{com}$	Set of communication edges
$\mathcal{L}$	Laplacian matrix
$\mathcal{L}^{com}$	Laplacian matrix of the communication network
$\mathcal{N}_i$	Set of nodes neighbouring node i
$\mathcal{V}$	Set of nodes

Alphabet

C_{ti}	Capacitance of DGU i
I_k^*	Current at power line k
I_{li}	Load demand at DGU i
I_{li}^*	Constant current load at DGU i
I_{ti}^*	Generated current at DGU i
K_i	Tuning parameter of DGU i
k_{ij}	Power line connecting DGU i and j
L_k	Inductance at line k
L_{ti}	Inductance at DGU i
m	Number of power lines in the network
m_c	Number of communication links in the network
n	Number of distributed generation units (DGUs) in the network
P_i	Power at source node i
P^*	Power convergence value
P_{li}^*	Constant power load at DGU i
R_k	Resistance at power line k

$T_{\theta i}$	Tuning parameter of DGU i
$T_{\phi i}$	Tuning parameter of DGU i
u_i	Control input
V	Vector of voltages
V_i	Voltage at PCC of DGU i
V^*	Reference voltage
W	Matrix of weights assigned to DGUs
w_i	Weight assigned to DGU i
Z^*_{li}	Constant impedance load at DGU i

Greek alphabet

Γ	Matrix of communication link weights
γ_{ij}	Weighted communication link connecting node i and node j
θ	Controller's state variable
ϕ	Controller's state variable

Chapter 1

Introduction

Economical, technological and environmental incentives are changing the face of electricity generation and transmission (Lasseter and Piagi, 2004). In the past years, many countries have begun the transition of their energy systems towards a more sustainable energy supply based on renewable energies. A trend is recognised that countries transforming their energy systems from a rather centralised approach with continuous energy generation based on fossil fuels to a more decentralised system with fluctuating energy generation from thousands of energy production facilities (e.g. wind, solar, and biomass) (DENA, 2019).
Centralized generation refers to the large-scale generation of electricity at centralized facilities. These facilities are usually located away from end-users and connected through a network of high-voltage transmission lines. The electricity generated by centralized generation is distributed through the electric power grid to multiple end-users. Centralized generation facilities include fossil-fuel-fired power plants, nuclear power plants, hydroelectric dams, wind farms, and more (EPA, 2018a).
On the contrary, a variety of small-scale technologies that generate electricity at or near where it will be used is referred as distributed generation (EPA, 2018b). Distributed generation of electricity offers numerous benefits in comparison to the conventional centralized systems. Important benefits of decentralized power generation systems are no high peak load shortages, reduced high transmission and distribution losses, linking remote and inaccessible areas, faster response to new power demands, and improved supply reliability and power management (ISGF, 2019).

Recent trends of increasing electricity demands for critical infrastructure have led to increasing interest in microgrids. Microgrids are defined as low-voltage distribution networks which comprise of various small-scale distributed generator units (DGUs), energy storage devices, and controllable loads that are connected through power lines. The small-scale generation units usually have a production capacity of 10 megawatts or less.
In contrary to traditional centralised power system, microgrids can can operate either in grid-connected mode, or in islanded mode. In grid connected mode, the microgrid decit power must be supplied by the main grid, and the excess power produced in the microgrid must be sent to the main grid (de Souza and Castilla, 2019). If the main grid supplies power to microgrid, the main power-grid acts as an controllable voltage source (Venkatraman and Khaitan, 2015). In island mode, the microgrid operates independently from the main grid (Arif and Hasan, 2018), for example in aircrafts and ships. These microgrids have many advantages over traditional energy distribution systems, like the increase in reliability, power quality improvement, and a reduction in distribution network losses (Rahmani et al., 2017).

Nowadays there exist several examples of small DC microgrids, as in marine, aviation, automotive, and manufacturing industries. In all these examples it is extremely important that the microgrid is controlled such a way that it presents reliability and proper operation. Microgrids should be

able to locally solve energy problems and hence increase flexibility (Guerrero et al., 2012a).
One of the main challenge to assure reliability, flexibility and proper operation of microgrids is the complex controllability of such a system (Rahmani et al., 2017). In a microgrid with multiple distributed generation sources, fair power sharing is an important aspect for the reliability of DGU in a microgrid. Fair power sharing means that the total demand of the microgrid is shared among all DGUs proportionally to the generation capacity of their corresponding energy sources. This control method prevents local generation units from exceeding their maximum generating capacity, to reduce maintenance cost and prevent for breakdown of DGUs which results in instability and unreliability of the power supply system. Besides, the autonomous operation of a microgrid requires local control strategies to maintain voltage at acceptable levels (Trip et al., 2014). Due to the increased interest in DC microgrids, the literature on DC microgrids from a control-theoretic perspective is rapidly growing. Many current, voltage and power sharing techniques, approached by different control strategies, are proposed literature.

1.1 Research problem and goal

As outlined in the previous section, reliability and the stability of the power power supply in a microgrid is important for numerous reasons. Especially when the microgrid operates in islanded mode, it is fully dependent of the power sources in the network. In order to increase the reliability and stability of a power system, power sources should be prevented for exceeding its generation limit, which can cause damage to distributed generation units and cause instability and unreliability of the power system. Therefore, DGUs in a microgrid should be controlled in such a way that the sources are prevented for exceeding their generation limit. Secondly, voltage regulation in DC microgrid is included, so that the voltages in the microgrid is maintained within acceptable limits.

This research aims to design a distributed control scheme that achieves fair power sharing and weighted average voltage regulation in dynamical DC microgrids. The power that is generated by every distributed generation unit (DGU) in a microgrid is proportional to the generation capacity of the corresponding DGU. In the microgrid considered in this thesis, multiple DGUs are interconnected through dynamic resistive-inductive (RL) power lines and supply so-called ZIP-loads i.e., nonlinear loads with the parallel combination of unknown constant impedance (Z), current (I) and power (P) components.
After a distributed control scheme that achieves fair power sharing is proposed, the performance of the control scheme analysed via extensive simulations in MATLAB. Critical and realistic scenarios are considered for simulations that include: various network topologies, plug-and-play scenarios and possible failure of power lines and communication scenarios.
After the proposed control scheme is analysed, interesting new insights regarding the design of a microgrid are provided, to improve the stability and reliability of such a system.

Therefore, the main objectives of this research are summarized in the following research goal:

Design a distributed control scheme that achieves fair power sharing and weighted average voltage regulation in DC microgrids, and analyse the performance of the proposed control scheme

1.2 Research questions

In order to reach the research goal in a structural manner, the following research questions (RQs) are posed:

RQ 1: What are the available control strategies to control DC microgrids?
This knowledge question provides prior knowledge of control strategies of DC microgrid, which is essential to design the control scheme

RQ 2: What are the mathematical tools required to develop the models in this thesis?
This knowledge question provides preliminaries required for the subsequent questions

RQ 3: How will a DC microgrid be modeled?
This design question provides the differential equations that describe the behaviour of the dynamical DC microgrid

RQ 4: How will the control scheme be modeled?
This design question provides the differential equations that describe the dynamical behaviour of the proposed distributed control scheme. Together with the differential equations of the DC microgrid, the dynamical behaviour of the overall system is described

RQ 5: What realistic and critical scenarios will be used to analyse performance of the proposed control scheme?
This design question provides under which realistic circumstances the control scheme is tested

RQ 6: How does the control scheme, that is proposed in this thesis, performs in critical circumstances?
This question provides an analysis of the performance of the control scheme

RQ 7: To what new insights lead the analysis of the proposed control scheme?
This question provides new insights with regard to the design of microgrids

RQ 8: What conclusions can be drawn from the analysis of the proposed distributed control scheme?
This knowledge question determines the main conclusions of the thesis, in order to add knowledge to existing literature, while also discussing current limitations and potential areas for further work

Answering the research questions mentioned above will result in achieving the research goal that is stated in section 1.1.

1.3 Thesis outline

The research questions posed above are generally answered in numerical order throughout the thesis. The remainder of this thesis is outlined as follows:

Subsequent to the introduction, chapter 2 covers the theoretical background of the thesis which forms the backbone of this work. The chapter discusses the current trends in power systems which supports the relevance of DC microgrids. Furthermore, current available control strategies of DC microgrids are discussed to provide understanding of control operations in DC microgrid. A control strategy from the available control strategy is chosen and justified which leads the rest of the thesis.

Secondly, in chapter 3 discusses the preliminaries for the remainder of the thesis. This chapter provides the tools that are used in models that are developed in the subsequent chapters, but could be skipped by the experienced reader. This chapter answers *research question 2*.

In chapter 4, a DC microgrid model is developed, using the tools that are discussed in chapter 3. This DC microgrid model is used to develop a control scheme for, which is predestined in the next chapter. This chapter answers *research question 4*.

In chapter 5, a distributed control scheme is designed that achieves fair power sharing among the distributed generation units (DGUs) the DC microgrid model that is developed in chapter 4. This chapter answers *research question 5*.

Subsequently, chapter 6 follows from chapters 4 and 5. In this chapter, the performance if the proposed distributed control scheme (designed in chapter 5) for the DC microgrid model (developed in chapter 4) is investigated through simulation of critical and realistic scenarios using MATLAB. These scenarios include variation of network topology, plug-n-play scenarios, failure of power lines and failure of communication between DGUs. Besides, from the simulation results, interesting new insights are determined. This chapter answers *research question 5, 6 and 7*.

Finally, *research question 8* is addressed in chapter 7, in which concluding remarks are provided and the thesis is concluded by discussing limitations of the current research project and highlighting potential areas for further work in chapter 8

Chapter 2

Theoretical background

This chapter provides a theoretical background on power networks, microgrids and the control of microgrids. The goal of this section is to provide a theoretical framework of the principles that are used in the rest of this work. *Research question 2* is answered in this chapter. In section 2.1 and section 2.2 theory and trends of power systems and microgrid systems is provided to emphasise the relevance of control of DC microgrids, not only now but but also in the future. In section 2.3, different control strategies that are currently available in literature are highlighted and the section elaborates on a control approach where the rest of thesis continuous on. *Research question 1* is answered in this chapter.

2.1 Power systems

The power network can be regarded as one of the most important infrastructures the world knows (Trip et al., 2020). The demand for electrical energy in the 21^{st} century is increasing worldwide and a fast development in the area of renewable energy sources is required to overcome the environmental issues related to the reduction of greenhouse gases (Rinaldi et al., 2017). Since the very beginning, it has been an issue of debate regarding the choice of alternating current (AC) or direct current (DC) as system of electrical power transfer (Datta et al., 2018).
According to the history perspectives, AC power network has been the standard choice for commercial energy systems (Justo et al., 2013). Traditionally, large-scale power generation at centralized facilities are usually located away from end-users (EPA, 2018b). Therefore, AC distribution is used intensively due to long distances power has to cover, because alternating current have ability to easily change the voltage level throughout the system (Datta et al., 2018). To distribute the power from generation over multiple consumers, the power is transformed to various (high) voltages levels, as shown in Figure 2.1 (Conejo and Baringo, 2018).

The primary reason to transform power to high voltage, is to increase transmission efficiency. However, voltage transforming stages in AC power system are inefficient and results in power losses (Setiawan et al., 2016b).

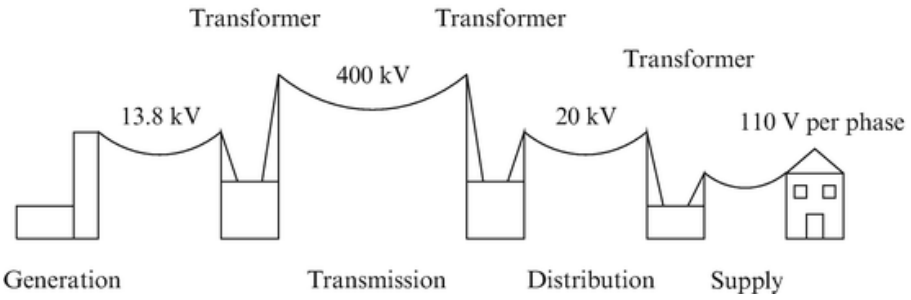

Figure 2.1: Physical layer of the AC power system (Conejo and Baringo, 2018)

On the contrary, distributed generation sources are usually located at, or near, the place where it will be used. Examples of distributed generation sources are photovoltaic cells and wind turbines. These are small-scale power sources, and have the ability to generate power near the consumer. Therefore, power does not have to cover long distances, and there is no need for voltage transforming stages. These advantages results in a higher efficiency rate of DC power systems of AC power systems.
Furthermore, power balance is a prerequisite in every power system. Power balance means that the production of power is equal to the power demand. Due to the stochastic nature (Mirakhorli and Dong, 2016), exactly predicting consumer power demand and power generation by renewable energy sources (such as wind and solar energy) is practically impossible. Besides, the current power AC power system is primarily designed for downstream power flow, yielding network security issues if local generation by renewable energy sources is too high.
These issues of debate has result in the increased interest in microgrids. A microgrid is the compressed version of the larger electrical grid that powers our country. In this small grid, the power demand in the grid is supplied by local sources and microgrid control ensures power balance in the network. Furthermore, microgrids are suitable for the integration of multiple renewable energy sources and high reliability provided adequate microgrid control.

2.2 Microgrid system

Microgrids can be categorised in three different categories: AC-, DC-, and hybrid- (combination of AC and DC) microgrids (Lotfi and Khodaei, 2015). Currently, most microgrids are AC driven, but DC microgrids show some major advantages compared to its counterpart due to its simpler control and the increase in reliability and efficiency (Jerin et al., 2018).

The advantages of DC microgrids compared to AC or hybrid microgrids, can be summarized as follow (Fei et al., 2019):

1. Most renewable energy resources, such as photovoltaic (PV) panels and fuel cells produce DC power. Even wind turbines, which intrinsically produce AC power, can be more conveniently integrated into a DC grid due to the absence of more power conversions.
2. There is no need for reactive power management and frequency synchronization.
3. Most of energy storage devices are also DC in nature. The battery technologies that are already provided with an internal DC-DC converter would be easily integrated to a DC bus with reduced cost and increased efficiency.

These important advantages that are stated above, result in the increased interest in DC microgrids over AC microgrids, where application of a DC microgrid can improve stability, reduce losses and enhance the flexibility of the power system.

As mentioned in the introduction, a microgrid refers to a set of distributed generation units (DGUs), control systems and loads that can independently supply the power required for the consumers with high reliability. (Beykverdi et al., 2017). Figure 2.2 shows a typical microgrid architecture that consist of power sources, storage capacity and loads.

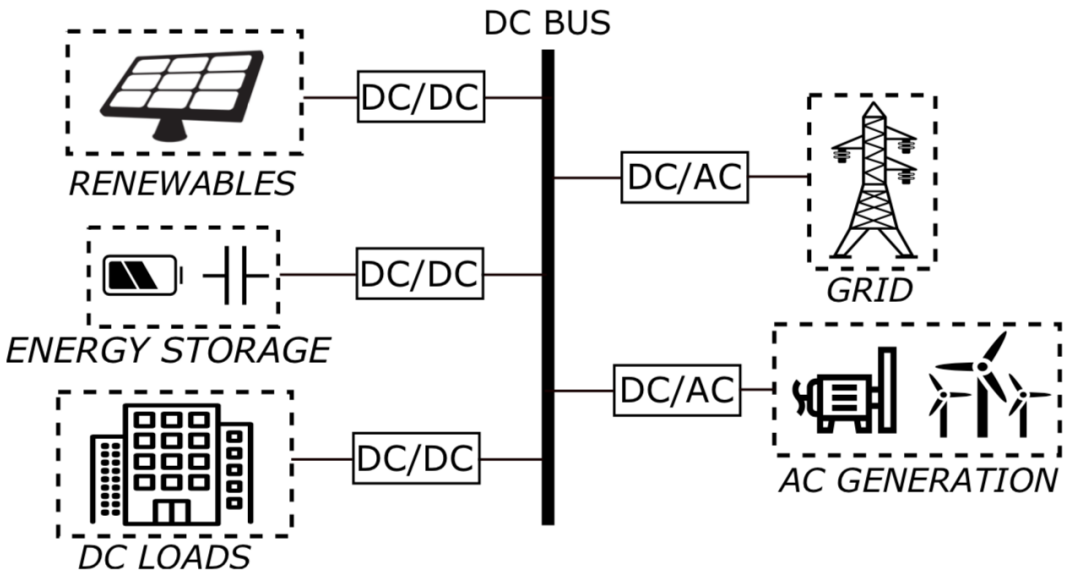

Figure 2.2: Typical microgrid architecture (Perez and Damm, 2019)

Power sources that are used in microgrids, such as photovoltaic panels, fuel cells, and battery banks operate in DC mode and are located near the loads. In addition, various loads such as computers, TVs, and LED bulbs are supplied with direct current (de Souza and Castilla, 2019), which eliminates power losses at conversion stages in a microgrid, since the supply and load are both in DC mode. However, not every power generator produces DC power, since most turbines (wind, hydro, or steam) produce AC power.

Renewable energy resources such as wind and solar are an important component of a microgrid. However, the inherent intermittency and variability of such resources complicates microgrid operations. Meanwhile, more loads, distributed generators (e.g., micro gas turbines and diesel generators), and distributed energy storage devices (e.g., battery banks) are being integrated into the microgrid operation (Su et al., 2013). Normally, the distributed energy storage system in a microgrid will only supply power when the total load demand exceeds the power generation capacity of DGUs in a microgrid (Beykverdi et al., 2017). In this thesis, the all power sources e.g. renewable energy sources, distributed generators and distributed energy storage systems are assumed to be controllable distributed generation units (DGUs), which implies that the intermittance of nature does not affect the power supply.

In general, a microgrid can have a schematic configuration as shown in Figure 2.3, where mulitple DGUs are connected to various loads through microgrid network. The microgrid is connected to the main grid at the point of common coupling (PCC). A microgrid is able to operate in grid connected operation mode (GCOM), or in islanded mode (IOM) i.e. when the microgrid is not connected to the main grid (Cucuzzella et al., 2018a). Several control techniques are reported in the literature to control microgrids either in GCOM or IOM (Incremona et al., 2016).
In grid-connected mode, the main grid can provide ancillary services to balance the supply and demand of power if the supplied power does not meet the load demand. When the microgrid is in

grid-connected mode. When the microgrid operates in island mode, the power that is generated within the microgrid, including the temporary power transfer from/to storage units, should be balanced with the total demand of the loads in the network. A DC microgrid in islanded operating mode is particularly interesting since IOS offer several promising advantages in reducing power losses, smoothly integrating RES and increasing the network resiliency (Cucuzzella et al., 2017). Besides, microgrids should preferably tie to the utility grid so that any surplus energy generated within the microgrid can be channeled to the utility grid (Guerrero et al., 2012b).

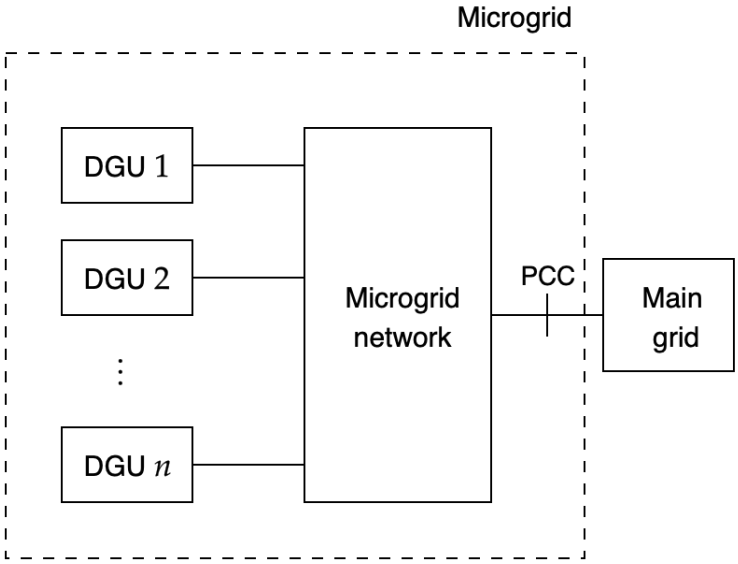

Figure 2.3: Schematic diagram of a generic microgrid with multiple DGUs

2.3 DC Microgrid control strategies

Advanced control strategies are vital components for realization of microgrids. It is extremely important that the microgrid is controlled such a way to present reliability and proper operation. To attain this goal, there are many control strategies. The most popular control technique is a linear control. It has gain its popularity due its simplicity and robustness. However as the name suggest, linear control considers a model that is linearized around an operating point. This implies that the simplified model is only valid around the operating point. Several approaches are available for linear control in microgrids. Examples are: transfer functions or state space modeling, where proportional integral derivative (PID), state feedback and linear–quadratic regulator (LQR) allocation of poles are viable strategies (Perez and Damm, 2019).
On the other hand, nonlinear control technique is based on the complete model of the system. This means the the nonlinear operation dynamics are included. The advantage of nonlinear control strategy is the more realistic grid modeling and that the model is not restricted to operate around the operating point. However a drawback of nonlinear control strategy is the increased complexity of analysis and the challenging implementation of the control law.

To ensure proper control of the microgrid, hierarchical control in different layers is implemented. These control layers provide certain degree of independence between different control levels. Besides, multiple control layers have the advantage to be more reliable as it continues to be operational even in the case of failure of the centralized control layer. (Fei et al., 2019). Figure 2.4 shows the three layers that are used in hierarchical microgrid control.

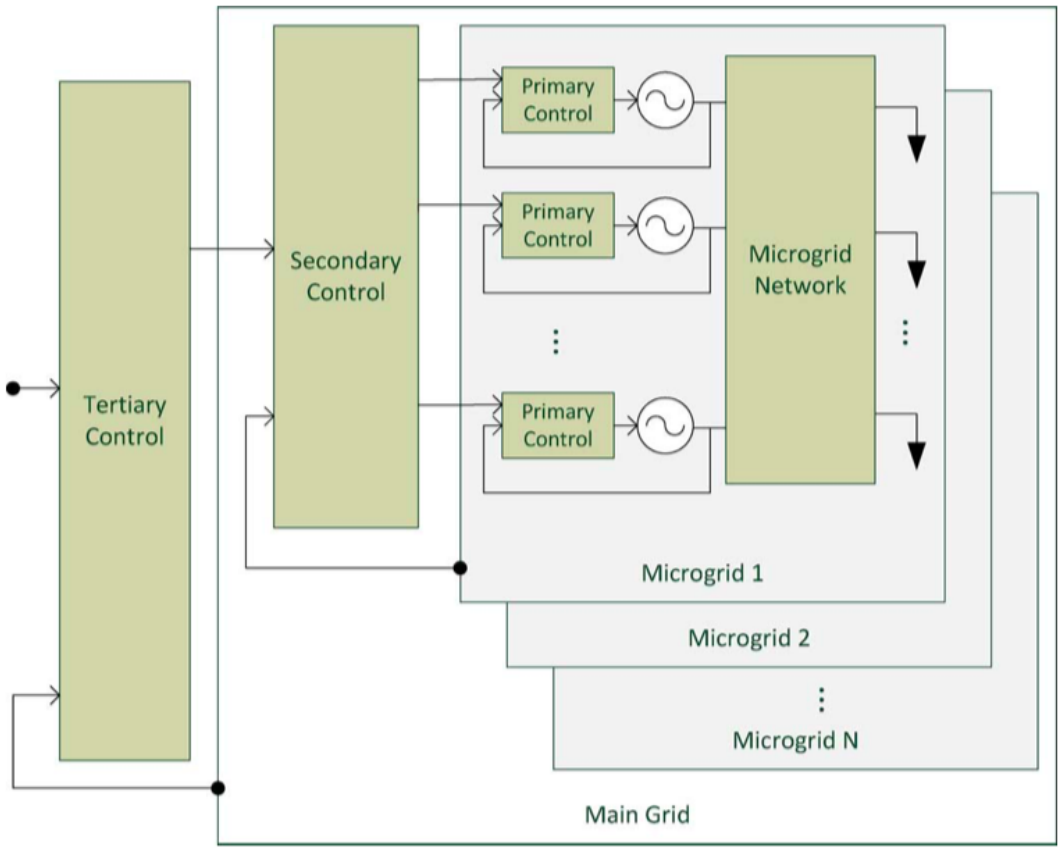

Figure 2.4: Hierarchical control layers of a microgrid (Olivares et al., 2014)

Conventionally, hierarchical control schemes are proposed to achieve current, voltage and power sharing (Fei et al., 2019). Figure 2.5 shows the hierarchical control architecture including primary, secondary and tertiary control level. The bandwidth, is the response time of the system. It is a measure of the time it requires to responds to a change of the input command. The figure shows that primary includes the fastest response time versus tertiary control which requires to most time to response to a change of variables within the system.

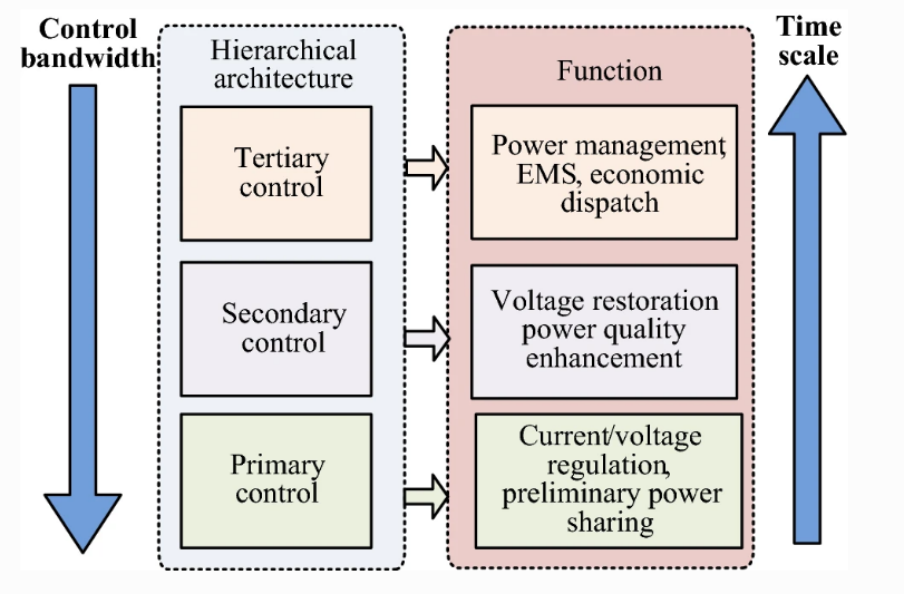

Figure 2.5: Hierarchical control architecture (Fei et al., 2019)

Primary control, also known as local control or internal control, is the first layer in the control hierarchy, including the fastest response. This control layer operates in a time range of a few seconds (Perez and Damm, 2019). The responsibility of the primary control layer is to regulate the current en voltage in the microgrid to adapt the grids operating points when disturbance acts on the system during the period the secondary controller requires to calculate the new set of optimal operation values.

Secondary control is responsible for the power quality. this implies the optimal power flow to ensure power balance in the system. This control layer regulates the power that is generated for each power source in the network. From a communication based perspective, the secondary control layer can be implemented in three different manners, as shown in Figure 2.6.

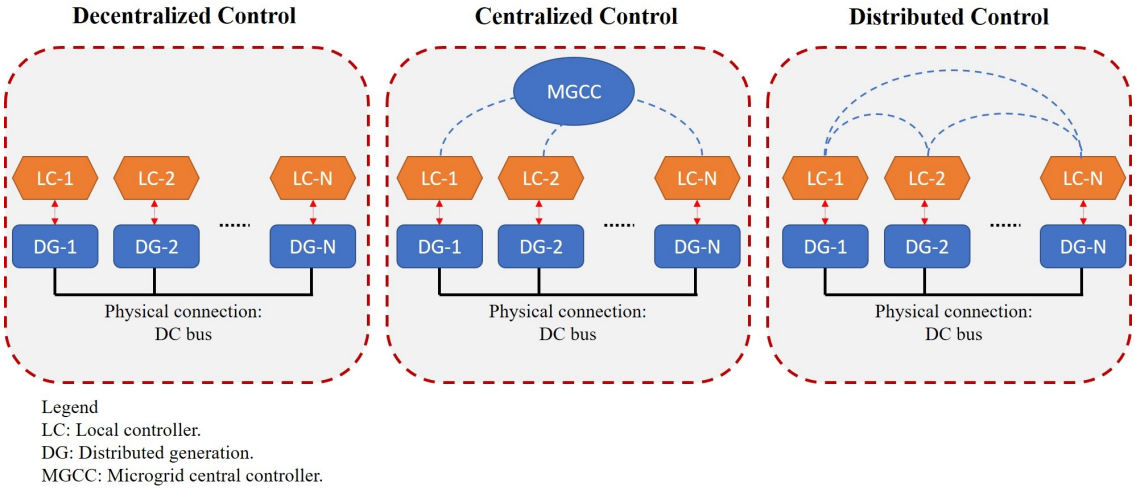

Figure 2.6: Three DC microgrid control methods (Saleh et al., 2018)

The different manners to implement the secondary control layer are shortly discussed below: (Saleh et al. (2018), Perez and Damm (2019))

In **decentralized control**, no communication is required. This control technique only uses measured local information to define its control actions. Therefore, all the DGUs can operate in parallel and are not depend of each other or of communication.

In **centralized control**, all sensors' data (e.g. microgrid states) is are transmitted from the DGUs to a central controller (MGCC). This central controller processes all the incoming data and sends back actions of control. Since the central controller has real-time data of all the power sources, it can reach or approach optimal performance of the microgrid. However, a drawback is that the controls reliability depends on the reliability of the communication network.

In **distributed control** no central controller is required. DGUs communicate their states only to their direct neighbours to achieve optimal performance. The main advantage of this method is that a DGU is only dependent of the communication between itself and its neighbours. Therefore, the system can maintain full functionality, even if the failure of some communication links occurs, provided that the communication network remains connected. This implies that distributed control is immune to a single point of failure (SPOF).

Finally, **tertiary control** is the highest layer in the hierarchy control scheme, including the slowest response time. This layer deals with the energy market, organizing the energy dispatch schedule according to an economic point of view, taking into account negotiation between consumers and producers. This level also deals with human–machine interaction and social aspects (Perez and Damm, 2019).

In order to design a control scheme that achieves fair sharing, which is a goal of this thesis, the control law is placed in the secondary layer of the hierarchical control scheme. The proposed control scheme is based on distributed control, since this control method has most potential to achieve high reliability and quality of the power supply in a microgrid due to its immunity for SPOF, local information sharing and low dependency.

Chapter 3

Preliminaries

This chapter provides a theoretical background on power system dynamics, presenting required preliminaries for the subsequent chapters. This chapter contains notation and concepts that are applied in the remainder of the research and answers *research question 3*.

3.1 Notation

Throughout this thesis, $\mathbb{N}$ and $\mathbb{R}$ denote the set of natural and real numbers, respectively. Furthermore, $\mathbf{1}_n \in \mathbb{R}^{n\times 1}$ denotes a column vector of ones, I_n denotes an identity matrix of size n, and $\circ$ denotes the Hadamard (entrywise) product.

Secondly, the calligraphic letters used in this research are reserved for the following matrices:

Table 3.1: Calligraphic letters and their matrices

Calligraphic letter	Matrix
$\mathcal{A}$	Adjacency matrix of a graph
$\mathcal{B}$	Incidence matrix of a graph
$\mathcal{D}$	Degree matrix of a graph
$\mathcal{L}$	Laplacian matrix of a graph
$\mathcal{L}^{com}$	Laplacian matrix of a communication graph

3.2 Electrical networks as graphs

In network theory, a DC power network is represented by a connected and undirected graph $\mathcal{G} = (\mathcal{V}, \mathcal{E})$. The graph consist of a set of nodes $\mathcal{V} = \{1, \ldots, n_v\}$, which represents the DGUs and a set of edges $\mathcal{E} = \{1, \ldots, n_e\}$, which represent the power lines interconnecting the DGUs.

The network topology is described by its corresponding incidence matrix that consist of $\mathcal{V} \in \mathbb{R}^n$ and $\mathcal{E} \in \mathbb{R}^n$, which relates nodes to their connected edges. The incidence matrix $\mathcal{B} \in \mathbb{R}^{n\times m}$. the labels are arbitrarily labeled with a $+$ and a $-$ where the entries of $\mathcal{B}$ are given by

$$\mathcal{B}_{i,k} = \begin{cases} +1 & \text{if node } i \text{ is connected to the positive end of edge } k \\ -1 & \text{if node } i \text{ is connected to the negative end of edge } k \\ 0 & \text{otherwise.} \end{cases} \tag{3.1}$$

Similarly, the communication network is represented by a connected and undirected graph $\mathcal{G}^{com} = (\mathcal{V}, \mathcal{E})$. The graph consist of a set of nodes $\mathcal{V} = \{1, \ldots, n_v\}$, which represents the DGUs and a set of edges $\mathcal{E} = \{1, \ldots, n_e\}$, which represent the communication lines interconnecting the DGUs. The incidence matrix for the communication network, $\mathcal{B}^{com} \in \mathbb{R}^{n \times m_c}$, describes the network topology nodes that communicate with each other.

$$\mathcal{B}^{com}_{i,k} = \begin{cases} +1 & \text{if node } i \text{ is connected to the positive end of communication edge } k \\ -1 & \text{if node } i \text{ is connected to the negative end of communication edge } k \\ 0 & \text{otherwise.} \end{cases} \tag{3.2}$$

In this research, the incidence matrices are used to model the power flow and communication between the nodes.

Chapter 4

DC Microgrid model

In this chapter, a DC microgrid model is developed to answer *research question 4*. The model is a typical DC microgrid model, which consist of n distributed generation units (DGUs) that are connected through m resistive-inductive (RL) power lines. Furthermore, m_c communication links connects DGUs. This does not necessarily mean that there is a communication link between every DGU, but it does mean that every DGU communicates with at least one other DGU. Therefore, the physical network topology can be different from the communication network topology.

A schematic representation of a DGU and RL-power lines that interconnect DGUs is given below:

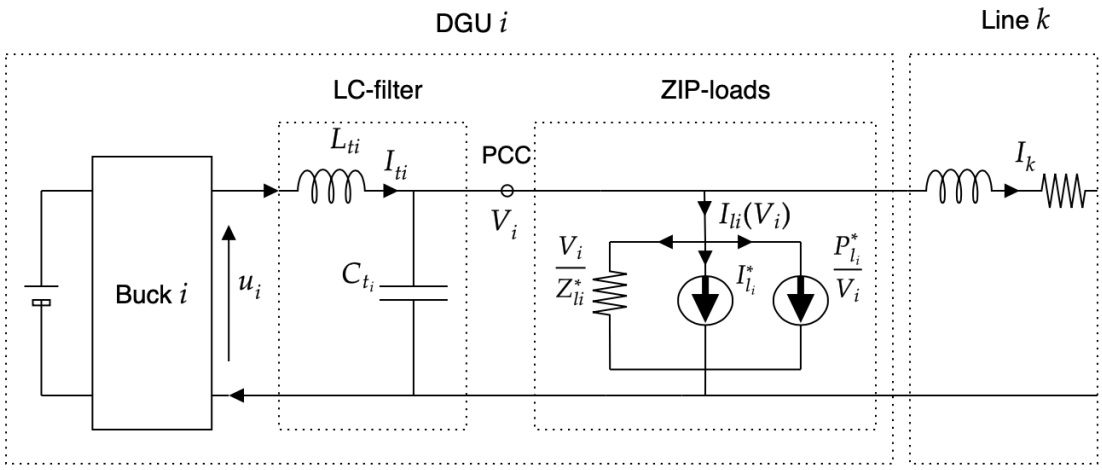

Figure 4.1: Schematic representation of DGU i and power line k

The symbols used in Figure 4.1, Equation 4.1 and Equation 4.3 are described in Table 4.1

Buck converter
The first element is typically an energy source of renewable type, which can be represented by a direct current (DC) voltage source. The DC voltage source supplies voltage to a DC buck converter. A buck converter (step-down converter) is a DC-to-DC power converter which steps down voltage, while stepping up current. Buck converters are usually highly efficient (> 90 %).
Due to this buck converter the voltage that is supplied to the loads can be controlled as an function of the current from the source. Variable u_i denotes the control input, in units of voltage. The dynamics of the buck are neglected.

Table 4.1: Description of the used symbols

	State variables
I_{ti}	Generated current
V_i	Load voltage
I_k	Line current
	Parameters
L_{ti}	Filter inductance
C_{ti}	Shunt capacitance
R_{ij}	Line resistance
L_{ij}	Line inductance
	ZIP-loads
Z^*_{li}	Constant impedance
I^*_{li}	Constant current
P^*_{li}	Constant power
	Inputs
u_i	Control input
I_{li}	Unknown current demand

LC-filter
The current supplies the loads via a LC filter, consisting of a inductor and a resistor. The inductor is placed in series and the conductor is is placed in parallel to the voltage source. The filter acts as a resonant which stores energy in the inductor and capacitor to damp oscillations, occurring in the circuit.

PCC
The point of common coupling (PCC) denotes the point where the DGU is connected to the main grid. In normal mode, the microgrid is connected to the utility grid. The utility grid acts as an DGU. When the microgrid operates in island mode, the microgrid is not connected to the main grid and now power is supplied via the point of common coupling. In Equation 4.1, the load currents (I_{li}) are located at the PCC of each DGU. This is generally obtained by a Kron reduction of the original network (Trip et al., 2018). The Kron reduction of networks is ubiquitous in circuit theory and related applications in order to obtain lower dimensional electrically-equivalent circuits (Dorfler and Bullo, 2012).

The equations describing the dynamical behaviour of DGU i, as depicted in Figure 4.1, are given by

$$L_{ti}\dot{I}_{ti} = -V_i + u_i \tag{4.1a}$$
$$C_{ti}\dot{V}_i = I_{ti} - I_{li} - \sum_{k\in\mathcal{E}_i} I_k \tag{4.1b}$$

Loads
In this research, a general nonlinear load model is considered that consist of three different type of loads. Loads in a power network can be broadly classified into two groups: nonactive and active loads. Common examples for nonactive loads are constant impedance (Z^*_l) loads and constant current (I^*_l), while constant power (P^*_l) is a active load (Cucuzzella et al., 2019a). The loads are placed in parallel as shown in Figure 4.2. A constant current load is a load that adjusts its resistant to maintain a constant current. A constant impedance load is a load that presents an unchanging impedance and a constant power load refers to a load that can maintain a constant input power regardless of the input voltage supplied. Constant power loads have a nonlinear relationship between input voltage and load current (Leonard, 2014). Due to the advancement in power electronics in the past decade, a considerable percentage of the loads consists of active loads (e.g. motor drives, power converters and electronic devices), which often behave as constant power loads (Cucuzzella et al., 2019a).

The ZIP-loads model denotes a parallel combination of the following components:

Z | constant impedance: $I_{li} = Z_{li}^{*-1} V_i$, with $Z_{li}^* \in \mathbb{R}_{>0}$

I | constant current: $I_{li} = I_{li}^*$, with $I_{li}^* \in \mathbb{R}_{\geq 0}$, and

P | constant power: $I_{li} = V_i^{-1} P_{li}^*$, with $P_{li}^* \in \mathbb{R}_{\geq 0}$

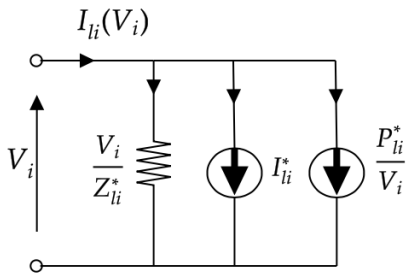

Figure 4.2: Schematic representation of the nonlinear load model that is considered in the DGUs

The total load demand (I_{li}) is the summation of the three loads when the loads are connected in parallel as shown in Figure 4.2. It is assumed that all the loads are not measurable. Accordingly, the presence of nonlinear ZIP-load in the DGU model, I_{li} in Equation 4.1b is given by:

$$I_{li}(V_i) := Z_{li}^{*-1} V_i + I_{li}^* + V_i^{-1} P_{li}^* \tag{4.2}$$

As mentioned in chapter 3, the overall DC microgrid system is modeled as an undirected graph $\mathcal{G} = (\mathcal{V}, \mathcal{E})$, with its corresponding incidence matrix $\mathcal{B} \in \mathbb{R}^{n \times m}$ to describe the network topology.

Consequently, the overall DC microgrid system can be written compactly as:

$$\begin{aligned} L_t \dot{I}_t &= -V + u \\ C_t \dot{V} &= I_t + \mathcal{B} I - (Z_l^{*-1} V + I_l^* + [V]^{-1} P_l^*) \\ L \dot{I} &= -\mathcal{B} V - R I \end{aligned} \tag{4.3}$$

Where $I_t, V, I_l, I_l^*, P_l^*, u \in \mathbb{R}^n$ and $I \in \mathbb{R}^m$. Furthermore, $C_t, L_t, Z_l^* \in \mathbb{R}^{n \times n}$ and $R, L \in \mathbb{R}^{m \times m}$ are positive definite diagonal matrices, e.g. $C_t = \text{diag}(C_{t_1}, \ldots C_{t_n})$

Moreover, $\overline{I}$, $\overline{I_t}$ and $\overline{V}$ are the steady state solutions to Equation 4.3 that satisfy the system of dynamics:

$$\overline{V} = \overline{u} \tag{4.4a}$$

$$\overline{I}_t = (Z_l^{*-1} \overline{V} + I_l^* + [\overline{V}]^{-1} P_l^*) - \mathcal{B} \overline{I} \tag{4.4b}$$

$$\overline{I} = -R^{-1} \mathcal{B}^\top \overline{V} \tag{4.4c}$$

At steady state condition, Equation 4.4a shows that the voltage supplied by the voltage source is equal to the control input u. Besides, Equation 4.4b shows that the current that generated current is equal to the current that is demanded by the loads together with the current that is flows through power lines to neighbouring nodes. Thirdly, the total current that flows through power lines to neighbouring nodes j, equal to the current leaving node i. Together, all three equations should hold to satisfy the steady state condition for the dynamics of the DGU model.

Chapter 5

Distributed control scheme

In this chapter, a distributed control scheme is designed which aims to achieves fair power sharing and average voltage regulation. *Research question 5* is answered in this chapter. To recall, fair power sharing means that every distributed generation unit in a DC microgrid generates the amount of power relative to its maximum production capacity and the maximum production capacity of DGUs in the network. Elementary, a power network contains a generator and consumers. To meet the consumers demand, the generator should produce as much power as the consumers use to achieve and maintain power balance in the power system. In reality, there are many consumers and also multiple producers (Weitenberg, 2018). Taken into account the increase popularity of solar panels and other renewable energy sources, many agents of the electrical distribution network are prosumers, playing an active role by producing and consuming energy (Cucuzzella et al., 2019b). There could be as many producers as consumers in a power network, each with a limited generation capacity. In fact, every power source has a limited capacity. This means that if someone turns on a machine that demands a lot of power, that load should be shared among the power sources. This motivates the consideration of power sharing, The simplest form of power sharing requires that each producer injects the same amount of power into the network at steady state. Of course, in reality, different power sources have different capacities. Therefore, we often aim for weighted power sharing instead, which gives each producer a weight, and balances the weighted power injections (Weitenberg, 2018).

5.1 Control objectives

As mentioned, the control scheme that is proposed in this chapter, aims to achieve fair power sharing and weighted average voltage regulation. The two objectives are discussed in this section.

5.1.1 Power sharing

The primary objective of the control scheme is to achieve fair power sharing at steady state. This implies weighted power sharing at steady state, since the weights corresponds to the power generation capacity of DGUs in the network, which are preset by the operator. The control objective is to guarantee that at steady state the following identities hold:

$$w_i P_i = w_j P_j, \quad \forall i, j \in \mathcal{V} \tag{5.1}$$

Where the power at a DGU i converges to its steady state solution for all $i \in \mathcal{V}$:

$$\lim_{t \to \infty} P_i(t) = \overline{P_i} \tag{5.2}$$

Where $\overline{P_i}$ is the the injected power at node i at steady state. According to Ohm's law, $\overline{P_i} = \overline{V_i}\ \overline{I_{ti}}$. Hence, P is the vector of power injections at the nodes. Therefore, the fair power sharing objective, can be written as an expression where the steady state power injections converge to a weighted power convergence value P^*:

$$\overline{P} = W^{-1}\mathbf{1}P^*, \quad P^* \in \mathbb{R} \tag{5.3}$$

with $W = \text{diag}(w_i, \ldots, w_n)$, $w > 0$ for all $i \in \mathcal{V}$ and P^* any scalar. To define an expression for P^*, Equation 5.3 is multiplied with $\mathbf{1}^\top$, to arrive at:

$$\mathbf{1}^\top \overline{P} = \mathbf{1}^\top [\overline{I_t}]\overline{V} = \mathbf{1}^\top W^{-1}\mathbf{1}P^* \tag{5.4}$$

After rewriting,

$$P^* = \frac{\mathbf{1}^\top [\overline{I_t}]\overline{V}}{\mathbf{1}^\top W^{-1}\mathbf{1}} \tag{5.5}$$

Besides, to obtain an expression for I_t, the steady state current balance in Equation 4.4b is multiplied with $\mathbf{1}^\top$:

$$\mathbf{1}^\top I_l = \mathbf{1}^\top I_t = Z_l^{*-1}\overline{V} + I_l^* + [\overline{V}]^{-1}P_l^* \tag{5.6}$$

Since $\mathbf{1}^\top \mathcal{B} = 0$. To this end, the power convergence value P^* is expressed as:

$$P^* = \frac{\mathbf{1}^\top ([Z_l^*]^{-1}[\overline{V}] + [I_l^*] + [\overline{V}]^{-1}[P_l^*])\overline{V}}{\mathbf{1}^\top W^{-1}\mathbf{1}} \tag{5.7}$$

It is observed that the steady-state injections Equation 5.2 achieves power sharing, and the asymptotic power value P^* to which the source power injections converge in a proportional fashion, is the total power injected divided by the weights. Therefore, when Equation 5.2 holds, the power at the DGUs converge to the reference power value and fair power sharing is achieved.

5.1.2 Average voltage regulation

The second objective is to achieve weighted average voltage regulation. Weighted average voltage regulation means that the weighted average of all DGUs in the network, converge to a preset reference voltage value (P^*), given as initial condition. Therefore, the weighted average value of V should converge to the weighted desired reference voltage value V^* at steady state. This results in the following objective where again the DGU with the largest capacity is assigned with the highest weight:

$$\lim_{t\to\infty} \mathbf{1}^\top W^{-1} V(t) = \mathbf{1}^\top W^{-1} \overline{V} = \mathbf{1}^\top W^{-1} V^* \tag{5.8}$$

The reason to include this objective is when power sharing is achieved, it does not necessarily mean that when fair power sharing is achieved, voltage levels at DGUs maintain within acceptable limits. Factors such as increased loading and distributed generation contribute to the difficulty in maintaining steady state voltages within prescribed limits (O'gorman and Redfern, 2004). Exceeding local voltage limits, can cause stability issues.

5.2 Control approach

In this section, a control scheme is designed that aims to achieve two objectives simultaneously. The primary objective is to achieve fair power sharing among all the DGUs in the network, as described in chapter 1. Besides, the second objective is weighted average voltage regulation of all the DGUs in the network.
In order to achieve weighted power sharing and average voltage regulation, the system is modeled with a feedback loop controller. As discussed in chapter 4, the system dynamics are described by three time dependent state variables, namely: voltage at PCC ($V_i(t)$), generated current ($I_{ti}(t)$) and exchange current ($I_i(t)$) for all $i \in \mathcal{V}$

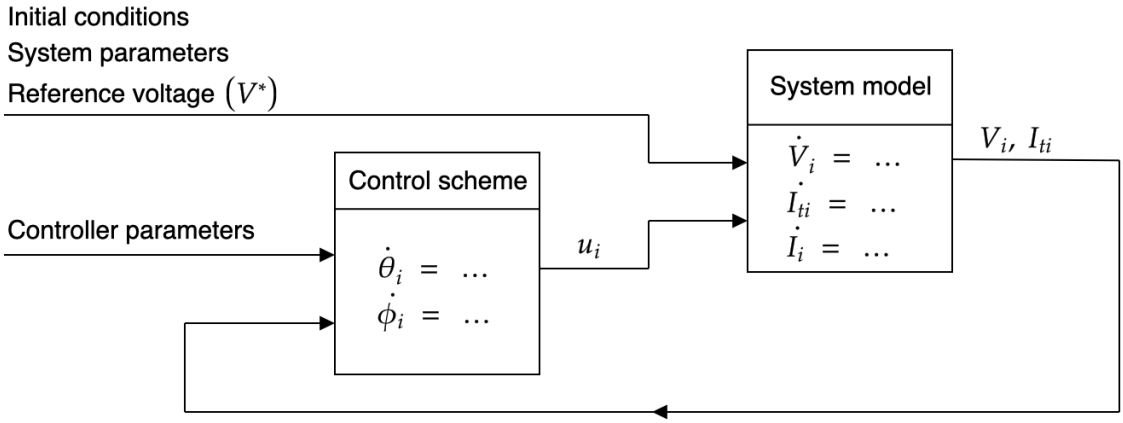

Figure 5.1: System model with feedback loop controller

As mentioned in chapter 4, the dynamics of the DC microgrid are described by three state variables, which are dependent of the system initial conditions and system parameters. As mentioned, the operator of the DC microgrid preset a reference voltage value where the weighted average voltage should converge to.
In order to achieve fair power sharing and weighted average voltage regulation, the control scheme is designed with two additional state variables, θ and ϕ, which can be tuned by controller parameters parameters (T_ϕ, T_θ). With use of the buck converter, the control input u is able to adjust the generated current as a function of voltage. Control input u is complemented with an tuning parameter K.

5.3 Distributed control scheme

However microgrid model that is considered in this research is fairly standard, the control scheme have some unique features compared to control schemes that are proposed in literature that achieves power, current, and voltage regulation (Weitenberg (2018), Cucuzzella et al. (2018b),

Tucci et al. (2018)). These unique featurs increase the applicability of the control scheme to control microgrids. The following features characterize the uniqueness of the proposed control scheme:

- resistive and inductive power lines are included, which increase the complexity of the system dynamics
- nonlinear ZIP-loads are included
- it is not needed to know the ZIP-load demands (Z_{li}^*, I_{li}^* and P_{li}^*). Only measurement of power (P_i) is required (i.e. measurement of voltage at PCC (V_i) and generated current (I_{ti}))
- the control scheme is independent of the initial conditions
- the topology of the communication network can be designed independently of the topology of the microgrid notwork
- the control scheme is independent of the microgrid parameters

The controller that is designed in this section is inspired by Trip et al. (2018), who propose a distributed control scheme that achieves current sharing and average voltage regulation. For the design of the control scheme, two assumptions are made. The first assumption is that the generated current (I_{li}) is measurable at the converter, and the voltage is measurable at the PCC of every DGU in the network. Secondly, it is assumed that there exist a reference voltage (V^*) for every DGU in the network that is preset by the operator.

The control scheme is proposed in the following manner:

$$\dot{\theta}_i = -\sum_{j\in\mathcal{N}_i^c} \gamma_{ij}\left(w_i I_{ti} V_i - w_j I_{ti} V_i\right) \tag{5.9a}$$

$$\dot{\phi}_i = -\phi_i + I_{ti} \tag{5.9b}$$

$$u_i = -K_i\left(I_{ti} - \phi_i\right) + w_i \sum_{j\in\mathcal{N}_i^{com}} \gamma_{ij}\left(\theta_i - \theta_j\right) + V_i^\star \tag{5.9c}$$

Where $\mathcal{N}_i^c$ denotes the set of DGUs which communicate with the i^{th} DGU. $\gamma_{ij} = \gamma_{ji} \in \mathbb{R}_{>0}$ are the weights of the communication links. $w_i, w_j \in \mathbb{R}_{>0}$ are the weights depending on the generation capacity of the DGU. Following the standard practise where the sources with the largest generation capacity determine the grid voltage, we select a weight of $\frac{1}{w_i}$ for all $i \in \mathcal{V}$. Let $\mathcal{L}^{com}$ denote the weighted Laplacian matrix of the communication network, which can be different from the Laplacian matrix of the physical network.

From Equation 5.9a, the the DC microgrid system is augmented with additional variable θ, which is a distributed integrator that is frequently used in distributed control schemes to achieve power or current sharing. Using $\mathcal{L} = \mathcal{B}^\top\mathcal{B} = \mathcal{D} - \mathcal{A}$, $\mathcal{L}^{com} = \mathcal{B}^{com\top}\Gamma\mathcal{B}^{com}$, where $\Gamma = \text{diag}(\gamma_{ij})$, and $W = \text{diag}(w_i)$, Equation 5.9a is rewritten in:

$$\dot{\theta} = -\mathcal{L}^{com} W (I_t \circ V) \tag{5.10}$$

Adding tuning parameters T_θ and T_ϕ result in a generic form:

$$\begin{aligned} T_\theta \dot{\theta} &= -\mathcal{L}^{com} W (I_t \circ V) \\ T_\phi \dot{\phi} &= -\phi + I_t \\ u &= -K(I_t - \phi) + W\mathcal{L}^{com}\theta + V^* \end{aligned} \tag{5.11}$$

The generated power $(I_t \circ V)$ and control state variable θ are exchanged to neighbouring nodes in the network. As mentioned, control input (u) represents an ideal voltage source that is controlled as a function of the local current I_{ti} and the injected power $P_j = V_j I_j$ at the neighbouring node sources $j \in \mathcal{N}_{c,i}$. Furthermore, the voltage source is designed for the local voltage to converge to a reference voltage V^*.

If the DC microgrid dynamics (Equation 4.3) and the control scheme dynamics (Equation 5.11) couple, the dynamics of the closed loop system arrive at:

$$L_t \dot{I}_t = -V - K(I_t - \phi) + W\mathcal{L}^{com}\theta + V^* \tag{5.12a}$$
$$C_t \dot{V} = I_t + \mathcal{B}I - (Z_l^{*-1}V + I_l^* + [V]^{-1}P_l^*) \tag{5.12b}$$
$$L\dot{I} = -\mathcal{B}^\top V - RI \tag{5.12c}$$
$$T_\theta \dot{\theta} = -\mathcal{L}^{com} W (I_t \circ V) \tag{5.12d}$$
$$T_\phi \dot{\phi} = -\phi + I_t \tag{5.12e}$$

5.3.1 Steady state

At the equilibrium, there exist a steady state solution $\left(\overline{I}_t, \overline{V}, \overline{I}, \overline{\theta}, \overline{\phi}\right)$ to the system described in Equation 5.12 that satisfy:

$$\mathbf{0} = -\overline{V} - K\left(\overline{I}_t - \overline{\phi}\right) + W\mathcal{L}^{com}\overline{\theta} + V^\star \tag{5.13a}$$
$$\mathbf{0} = \overline{I}_t + \mathcal{B}\overline{I} - (Z_l^{*-1}\overline{V} + I_l^* + [\overline{V}]^{-1}P_l^*) \tag{5.13b}$$
$$\mathbf{0} = -\mathcal{B}^\top \overline{V} - R\overline{I} \tag{5.13c}$$
$$\mathbf{0} = -\mathcal{L}^{com} W (\overline{I}_t \circ \overline{V}) \tag{5.13d}$$
$$\mathbf{0} = -\overline{\phi} + \overline{I}_t \tag{5.13e}$$

In the rest of this work, it is assumed that such a steady state exists. From the assumption that a steady state solution to the system of dynamics exists, the design of the control scheme is further substantiated.

From Equation 5.16 follows that at steady state $\overline{\phi} = \overline{I_t}$. Then, Equation 5.13a results in:

$$\mathbf{0} = -\overline{V} + W\mathcal{L}^{com}\overline{\theta} + V^\star \tag{5.14}$$

Multiply both sides with $\mathbf{1}^\top W^{-1}$ and after rewriting, Equation 5.15 shows that the voltage at PCC of the node converge to the desired reference voltage at steady state.

$$\mathbf{1}^\top W^{-1}(\overline{V} - V^*) = 0 \tag{5.15}$$

Therefore, the weighted average voltage control objective is achieved when the voltage converges to its steady state solution:

$$\lim_{t\to\infty} \mathbf{1}^\top W^{-1} V(t) = \mathbf{1}^\top W^{-1}\overline{V} = \mathbf{1}^\top W^{-1} V^* \tag{5.16}$$

Chapter 6

Simulations

In order to analyse the control of the DC microgrid model that is developed in chapter 4, by the distributed control scheme that is designed in chapter 5, extensive simulations are conducted to investigate the performance of the control scheme. To ascertain that the distributed control scheme achieves two objectives that are mentioned in chapter 5, different critical scenarios are considered that are based on realistic events. In section 6.5, interesting insights are provided regarding the design of microgrids as a result of the performance analysis of the control scheme.

The following scenarios simulated and the results are analysed to determine if the control scheme achieves the fair power sharing objective and weighted average voltage regulation objective:

1. **Benchmark network**
   In this scenario, the control scheme is applied to a benchmark network topology that consist of six DGUs that is widely used in literature to test current and power sharing controllers
2. **Power line failure**
   In this scenario, three possible power line failure scenarios are simulated to investigate the performance of the control scheme if power line failure occurs
3. **Communication line failure**
   In this scenario, the event of failure of a communication line between two nodes is simulated, to investigate if a DGU is not able to communicate with other DGUs in the network
4. **Plug-and-Play**
   In this scenario, the event of plug in, or plug out a DGU in DC microgrid network is simulated to analyse if the control scheme is robust for network topology changes. Plug-and-Play is an essential property of microgrids

To simulate the scenarios, MATLAB is used. The system parameters are inspired by parameters values that are found in literature. The following parameters remain equal throughout all the simulations that are conducted and therefore presented in Table 6.1

Table 6.1: Parameter values that remain unchanged during simulations

Parameter		Value
γ_{ij}	Weights of communication line connecting DGU i and j	100
T_θ	Tuning parameter of controller	1
T_ϕ	Tuning parameter of controller	1×10^{-2}
K	Tuning parameters of control input	0.5

6.1 Benchmark network

Firstly, the DC microgrid network topology that is considered for simulation is inspired by the benchmark network that is adopted in the European Union project "Microgrids" and proposed by (Papathanassiou et al., 2005).

The network consist of six distributed generation units ($n = 6$) that are connected through six power lines (distribution lines) ($m = 6$) and six communication lines ($m_c = 6$) that are connected via a DC bus to the main grid at the point of common coupling (PCC) in the following topology:

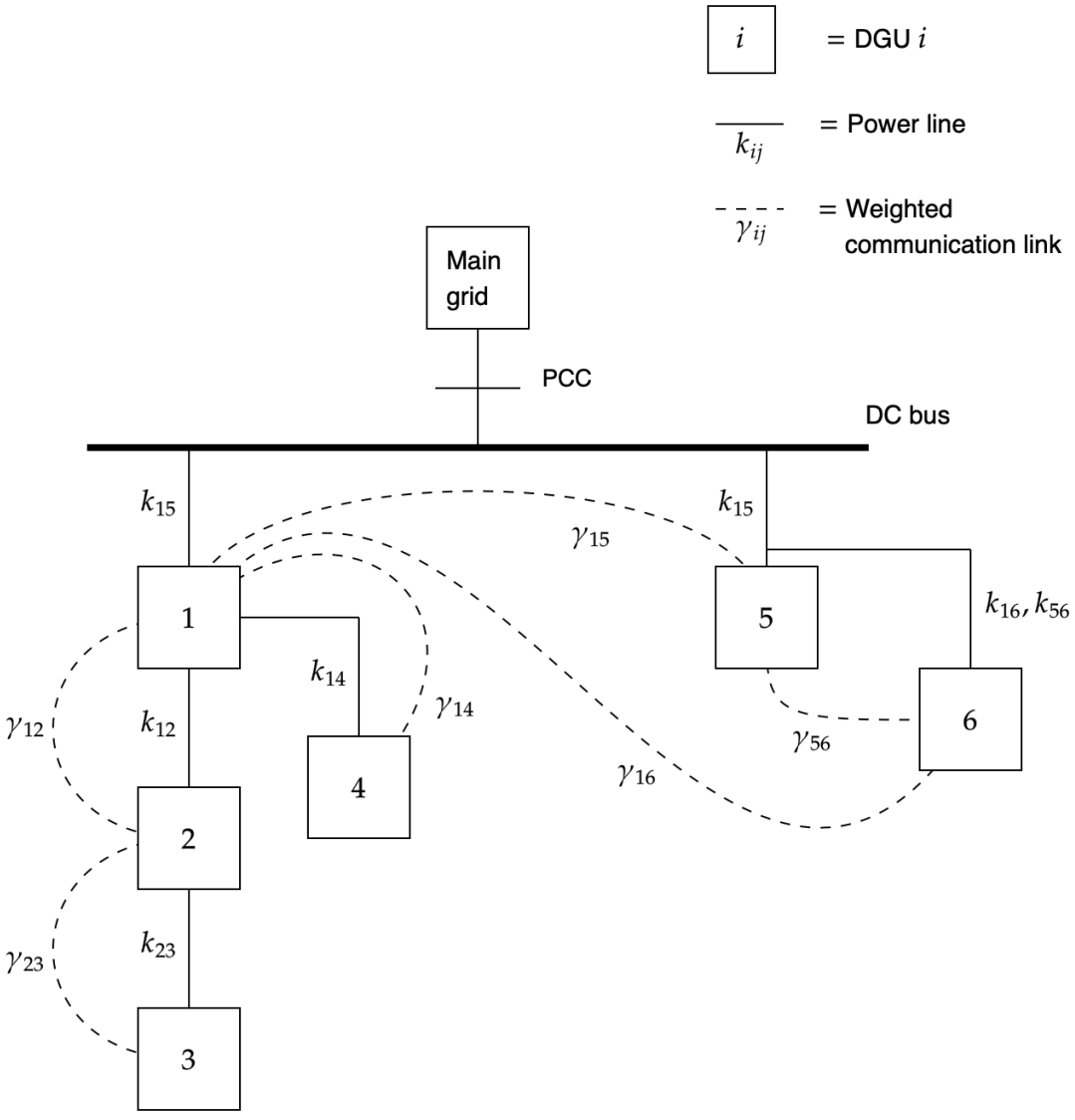

Figure 6.1: Schematic representation of the benchmark microgrid

The microgrid parameters can be found in Table 6.2, whereas the line parameters can be found in Table 6.3.

Table 6.2: DGU parameters of the benchmark network

DGU		1	2	3	4	5	6
L_{ti}	(mH)	1.8	2.0	3.0	2.2	2.1	1.7
C_{ti}	(mF)	2.2	1.9	2.5	1.7	2.4	1.8
W_i	(−)	0.3^{-1}	0.1^{-1}	0.05^{-1}	0.15^{-1}	0.22^{-1}	0.18^{-1}
$V_i^\star$	(V)	380.0	380.0	380.0	380.0	380.0	380.0
$I_{li}^*(0)$	(A)	30.0	15.0	30.0	26.0	35	10
$\Delta\ I_{li}^*$	(A)	+10	+7	-10	+5	-10	+5
$Y_{li}^*(0)$	(mS)	3.08	3.08	3.08	3.08	3.08	3.08
ΔY_{li}^*	(mS)	-0.5	-0.5	-0.5	-0.5	-0.5	-0.5
$P_{li}^*(0)$	(kW)	7.8	7.8	7.8	7.8	7.8	7.8
ΔP_{li}^*	(kW)	+1	+1	+1	+1	+1	+1

Table 6.3: Line parameters of the benchmark network

Line		{1,2}	{1,4}	{1,5}	{1,6}	{2,3}	{5,6}
R_{ij}	(mΩ)	70	50	80	60	80	40
L_{ij}	(μH)	2.1	2.3	2.0	1.8	2.3	2.1

A simulation is conducted for $0.2s$. At time instant $t = 0.1s$, load variations in constant impedance (ΔZ_{li}^*), constant current (ΔI_{li}^*) and constant power (ΔP_{li}^*) are considered when the system is at steady state (see Table 6.2). During a change in the load demand, the voltage at various load points has to be maintained within acceptable limit (e.g. 5% of the nominal voltage) (Setiawan et al., 2016a). In order investigate the performance of the control scheme, it is evaluated on its ability to achieve power sharing and average control regulation, which are two control scheme objectives stated in chapter 5.

6.1.1 Power sharing

To analyse the behaviour of the control scheme, the results are plotted to validate that the control scheme achieves power sharing. Figure 6.2 shows the power ($P_i(t) = I_{ti}(t)V_i(t)$) at the six nodes of the benchmark network. The power at the nodes differ according to the weights assigned to the DGUs. It is observed that the power at the nodes changes value if deviation in load demand occurs at $t = 0.1s$. Figure 6.2 shows that the power at node 1 encounters the highest power increase when load demand variation occurs, since the highest weight is assigned to node 1, because it is considered that DGU 1 has the highest generation capacity of all the DGUs in the network.

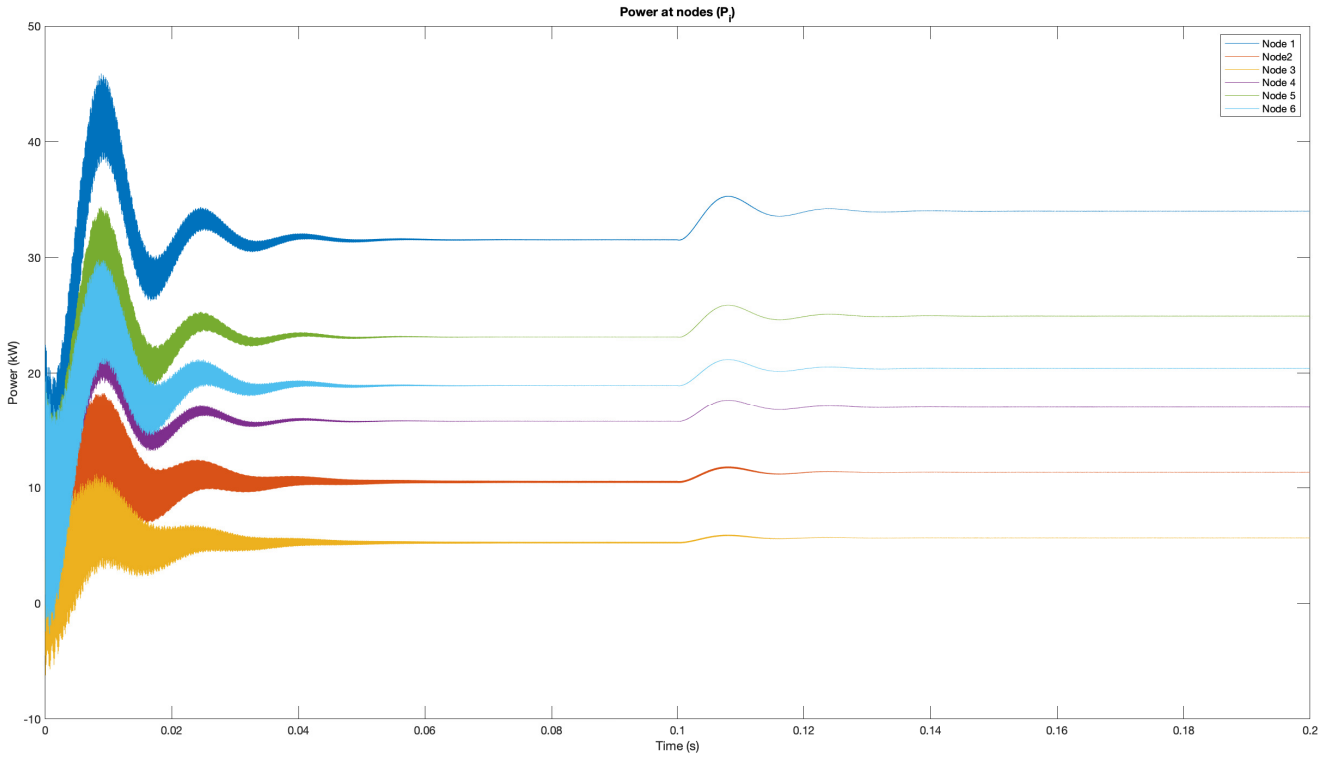

Figure 6.2: Power at node $i = 1, \ldots, 6$

However, to determine if the power is fairly shared among all the DGUs in the network, Figure 6.3 shows the result of the power at the nodes unconditionally of the weights assigned to the nodes. In other words, Figure 6.3 shows a plot of the result of $W_i(I_{ti}V_i)$ for all $i \in \mathcal{V}$.

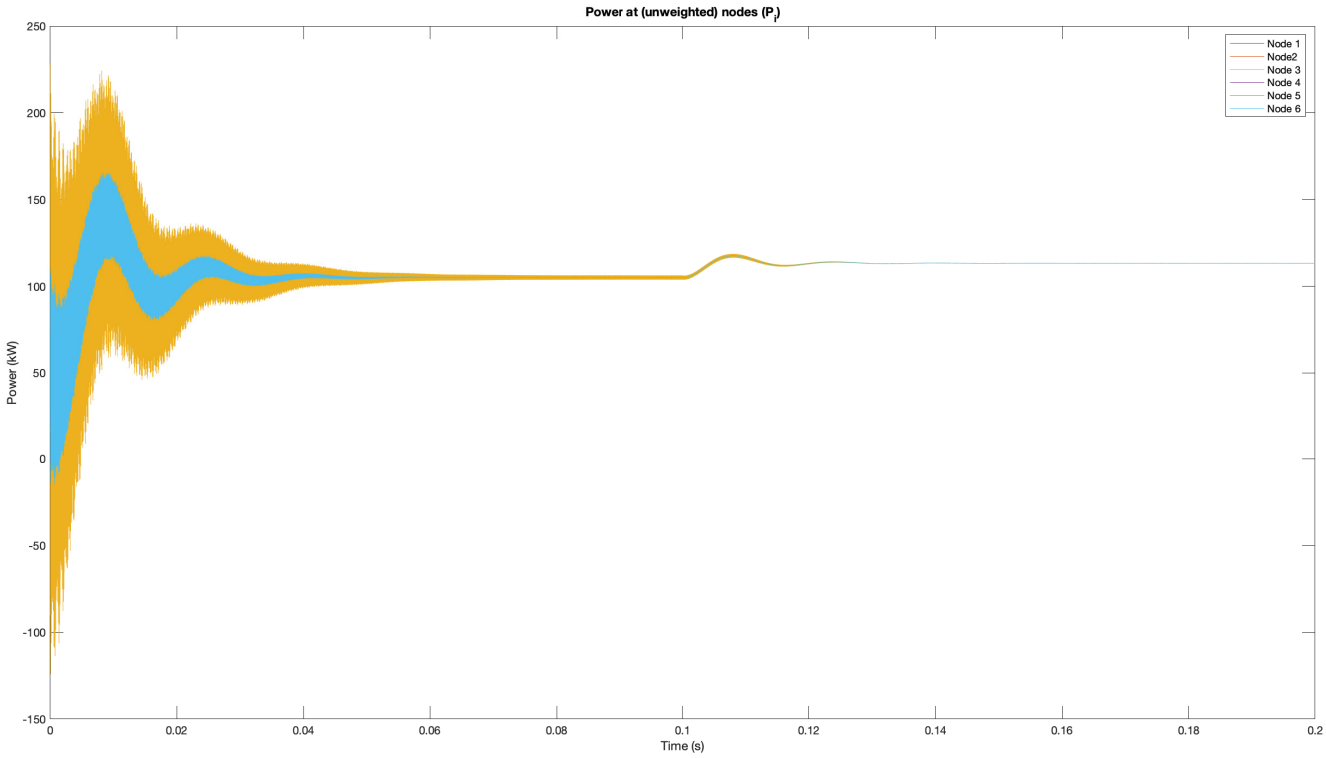

Figure 6.3: Fair power sharing among DGUs in benchmark network

Figure 6.3 shows that power sharing is achieved, since the power at DGUs at steady state are reaching a power consensus value to which the power at all the nodes in the network converges. The figure shows that $\overline{P} = P^*$ holds. Besides, the control scheme is robust load demand variation, which simulated at $t = 0.1s$.

6.1.2 Average voltage regulation

The second objective mentioned in chapter 5 is to achieve weighted average voltage regulation. This objective aims to control the weighted average voltage of the all the nodes in the network. This means that the weighted average voltage of all the nodes, converge to a reference voltage value (V^*) which is preset by the operator.

Figure 6.4 shows the voltage ($V_i(t)$) at the six nodes of the benchmark network. The voltage at the nodes differ according to the weights assigned to the DGUs. It is observed that the power at the nodes changes value if deviation in load demand occurs at $t = 0.1s$. Besides, Figure 6.4 shows that that the control scheme not not aims to achieve voltage sharing, since local voltages change independently of the weights assigned to the DGUs.

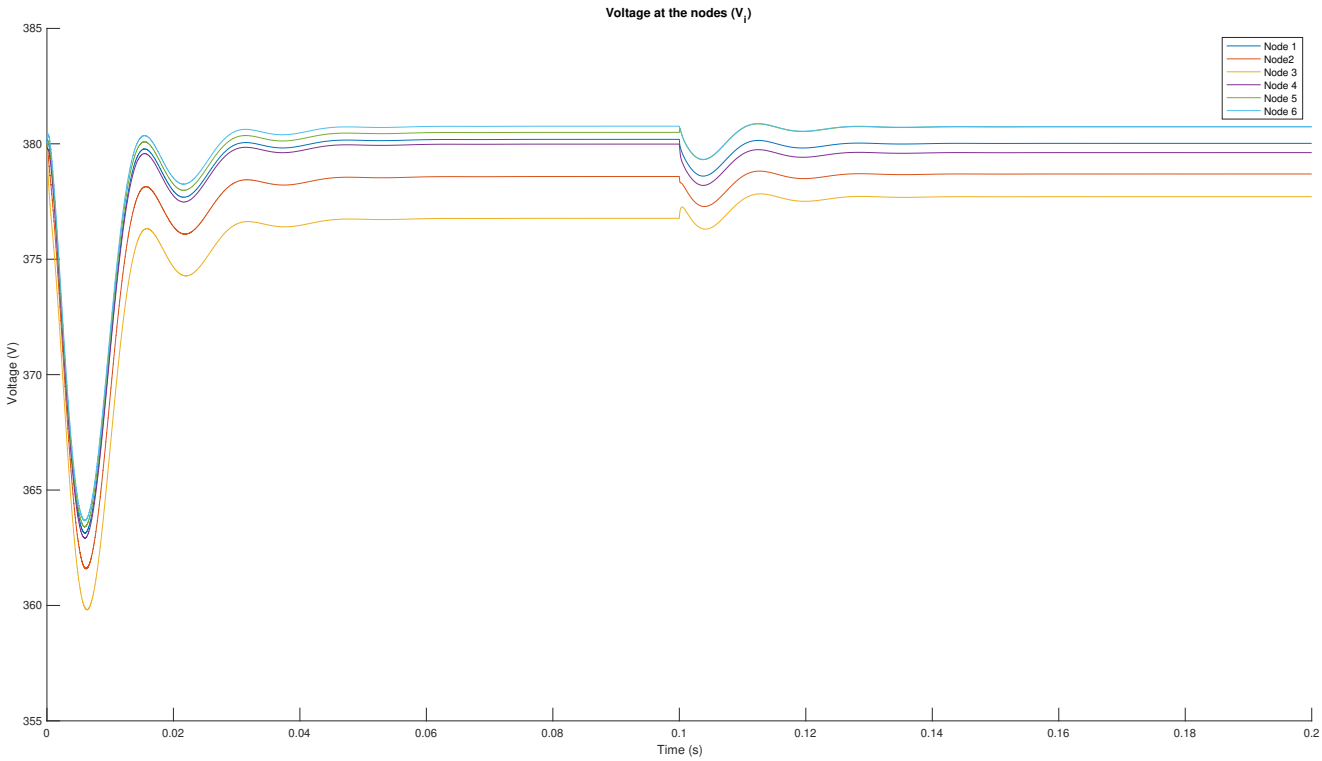

Figure 6.4: Voltage at DGU $i = 1, \ldots, 6$

However, to determine if weighted average voltage regulation in the microgrid is achieved, Figure 6.5 plots the weighted average voltage of the DGUs in the network that is defined by $V_{avg} = \mathbf{1}^\top W^{-1} V(t)$. Furthermore, the reference voltage (preset to 380V) is plotted, to determine if the weighted average voltage converges to the preset reference voltage value.

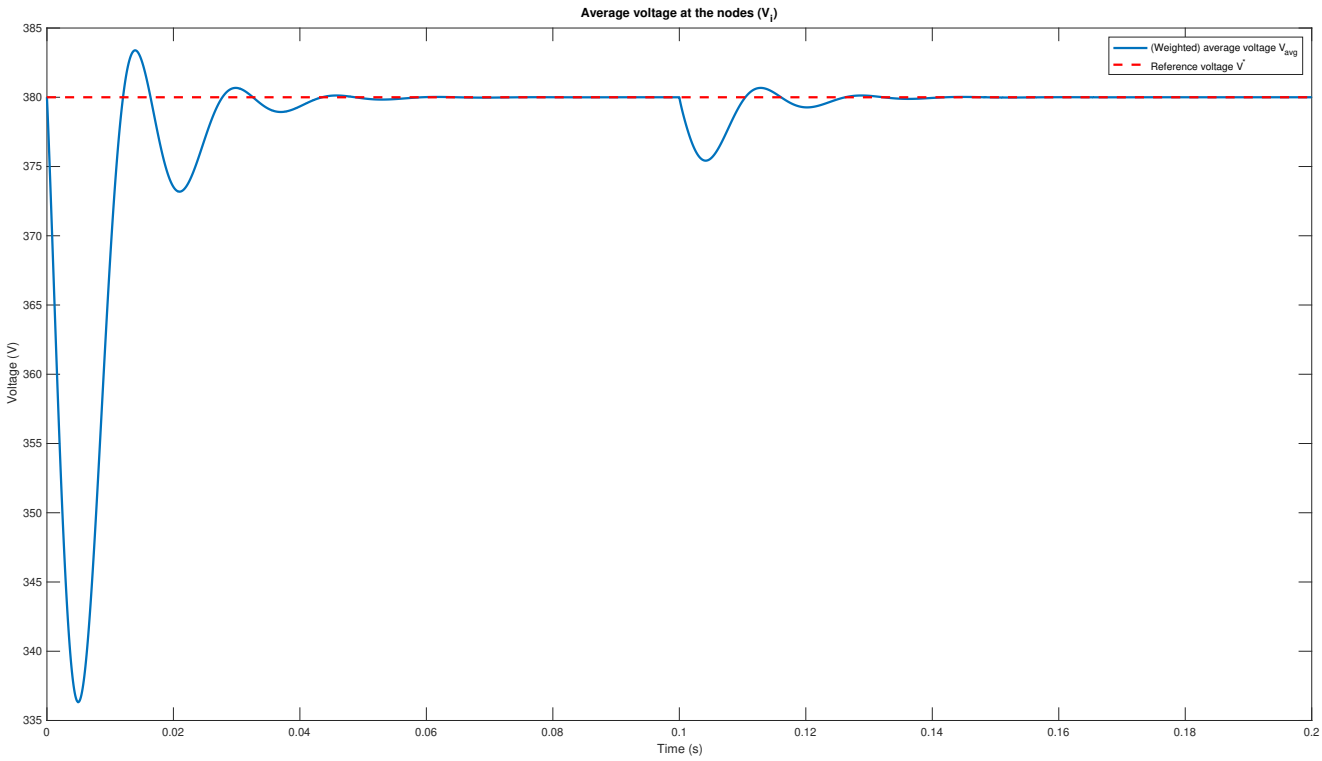

Figure 6.5: Average voltage regulation

Figure 6.5 shows that at steady state the weighted average voltage V_{avg} converge to the reference voltage V^*. Therefore, weighted average voltage regulation is achieved in the benchmark network ($\mathbf{1}^\top W^{-1} \overline{V} = \mathbf{1}^\top W^{-1} V^*$). After the load demand varies, the the convergence time is less, than initially. Also, under- and overshoot are of lower magnitude. The reason for this is that the load demand variation is relatively small, Therefore, the states before variation in load demand are near the steady values.

6.2 Power line failure

In the second series of scenarios, failure of different power lines are simulated. There are numerous reasons that can cause power line failure in electricity network, such as damage to power cables or joints.

A network is considered with four DGUs ($n = 4$), four power lines ($m = 4$) and three communication links ($m_c = 4$) in the following topology, with corresponding DGU parameter values described in Table 6.4 and line parameters in Table 6.5:

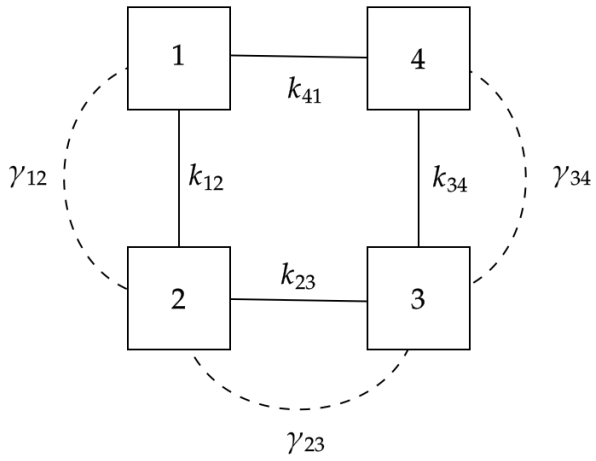

Figure 6.6: A schematic representation of a four DGU microgrid network that is considered for the simulation of the next series of scenarios

Table 6.4: DGU parameters of the four node network

DGU		1	2	3	4
L_{ti}	(mH)	1.8	2.0	3.0	2.2
C_{ti}	(mF)	2.2	1.9	2.5	1.7
W_i	$(-)$	0.4^{-1}	0.2^{-1}	0.15^{-1}	0.25^{-1}
$V_i^\star$	(V)	380.0	380.0	380.0	380.0
$I_{li}^*(0)$	(A)	30.0	15.0	30.0	26.0
$Y_{li}^*(0)$	(mS)	3.08	3.08	3.08	3.08
$P_{li}^*(0)$	(kW)	7.8	7.8	7.8	7.8

Table 6.5: Line parameters of the four node network

Line		{1,2}	{2,3}	{3,4}	{4,1}
R_{ij}	(mΩ)	70	50	80	60
L_{ij}	(μH)	2.1	2.3	2.0	1.8

In the network of Figure 6.6, three identical power line failure scenarios can be identified, which result in ad hoc networks. Ad hoc electrical networks are formed by connecting power sources and loads without planning the interconnection structure (topology) in advance (Cavanagh et al., 2017). Therefore, the following three scenarios are simulated.

1. Failure of power line k_{41}
   Power line k_{41} denotes the line connection node one and node four. This line connects two nodes, where there is no communication link between the nodes.

2. Failure of power line k_{12}
   The second possible power line failure occurs when power line k_{12} fails. This power line connects two nodes where there is a communication link between the nodes (γ_{12}). This scenario is identical for power lines k_{23} and k_{34}

3. Failure of power lines k_{12} and k_{41} − isolation of DGU 1
   The third power line failure scenario occurs when two power lines fail simultaneously and isolate a node. However this DGU is not connected by power lines to the other DGUs, it still communicates with DGU 2 by communication link γ_{12}

The performance of the control scheme is investigated regarding power sharing and weighted average voltage regulation.

6.2.1 Failure of power line k_{41}

in the first power line failure scenario, the performance of the control scheme is investigated if a power line fails, when the two nodes do not directly communicate with each other. In Figure 6.7, the power line that fails is marked in red.

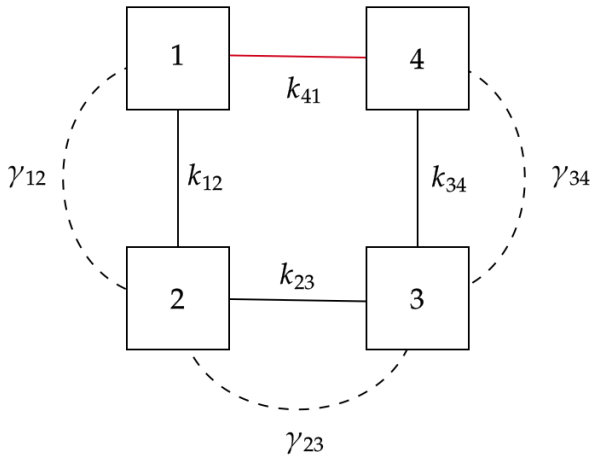

Figure 6.7: Failure of power line k_{41}

The power line failure is simulated at $t = 0.1s$, when the the system is initially at steady state condition. In this scenario, the load demand does not change, as was the case during the simulation of the benchmark network in section 6.1.

The DGU parameters and line parameter can be found in Table 6.6 and Table 6.7 respectively.

Table 6.6: DGU parameters during failure of power line k_{41}

DGU		1	2	3	4
L_{ti}	(mH)	1.8	2.0	3.0	2.2
C_{ti}	(mF)	2.2	1.9	2.5	1.7
W_i	$(-)$	0.4^{-1}	0.2^{-1}	0.15^{-1}	0.25^{-1}
$V_i^\star$	(V)	380.0	380.0	380.0	380.0
$I_{li}^*(0)$	(A)	30.0	15.0	30.0	26.0
$Y_{li}^*(0)$	(mS)	3.08	3.08	3.08	3.08
$P_{li}^*(0)$	(kW)	7.8	7.8	7.8	7.8

Table 6.7: Line parameters after failure of power line k_{41}

Line		{1,2}	{2,3}	{3,4}
R_{ij}	(mΩ)	70	50	80
L_{ij}	(μH)	2.1	2.3	2.0

As shown in Figure 6.8, the current flow of power line k_{41} decreases to zero current flowing across that edge. Besides, the current flow across the other power lines changes, which implies that the current takes a "new route" to meet the load demands of all the nodes in the network. Negative current flow means that the current flows in the reversed direction than initialised by the incidence matrix. Clearly, the failure of power line k_{41} increases the peak load of the power lines which might cause stability issues if the current flow across the power lines exceeds the power line maximum capacity.

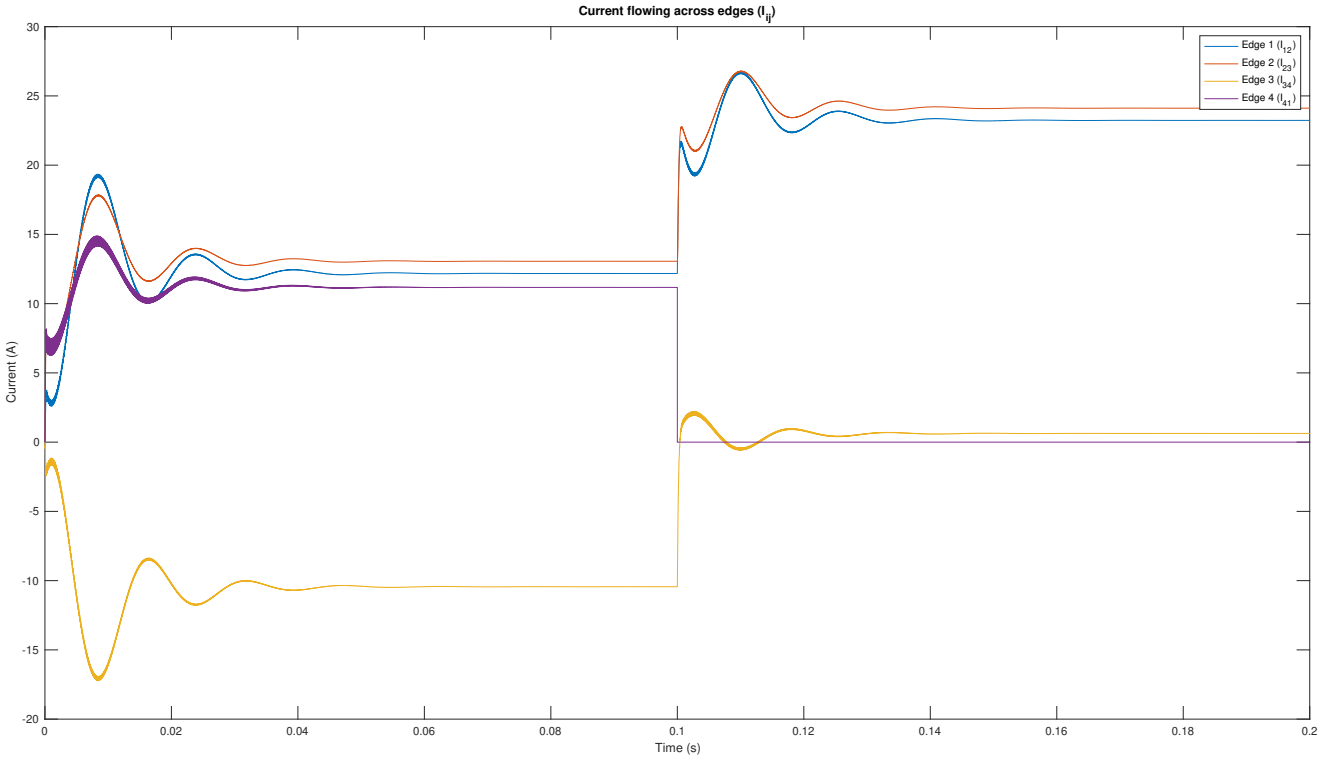

Figure 6.8: Current flow across edges during failure of power line k_{41}

Power sharing

In order to determine if power sharing is still achieved, Figure 6.13 shows a plot of the result of "unweighted" power at the nodes. "Unweighted" power means that the power at each node is compensated for its assigned weight.

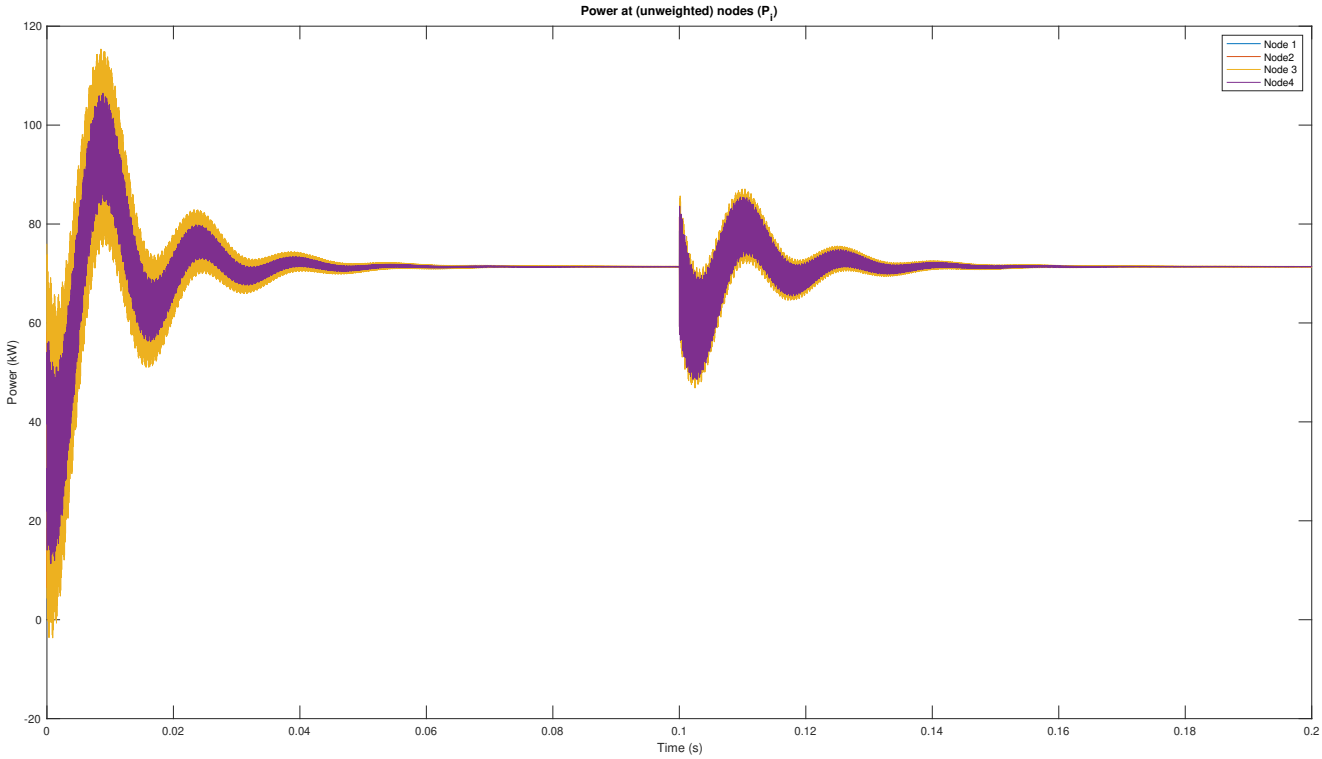

Figure 6.9: Fair power sharing among nodes during failure of power line k_{41}

Figure 6.13 shows that power sharing is achieved if power line k_{41} fails during operation of the microgrid. As expected, the control scheme requires time to find a new power consensus value. despite the power line topology, the parameters remain identical. Therefore, the unweighted power at the nodes converge to the same power consensus value P^* as prior to the power line failure.

Average voltage regulation

In order to determine if weighted average voltage regulation is still achieved, Figure 6.10 plots the result of the weighted average voltage of node $i = 1 \dots 4$ and the reference voltage V^* which is preset by the operator.

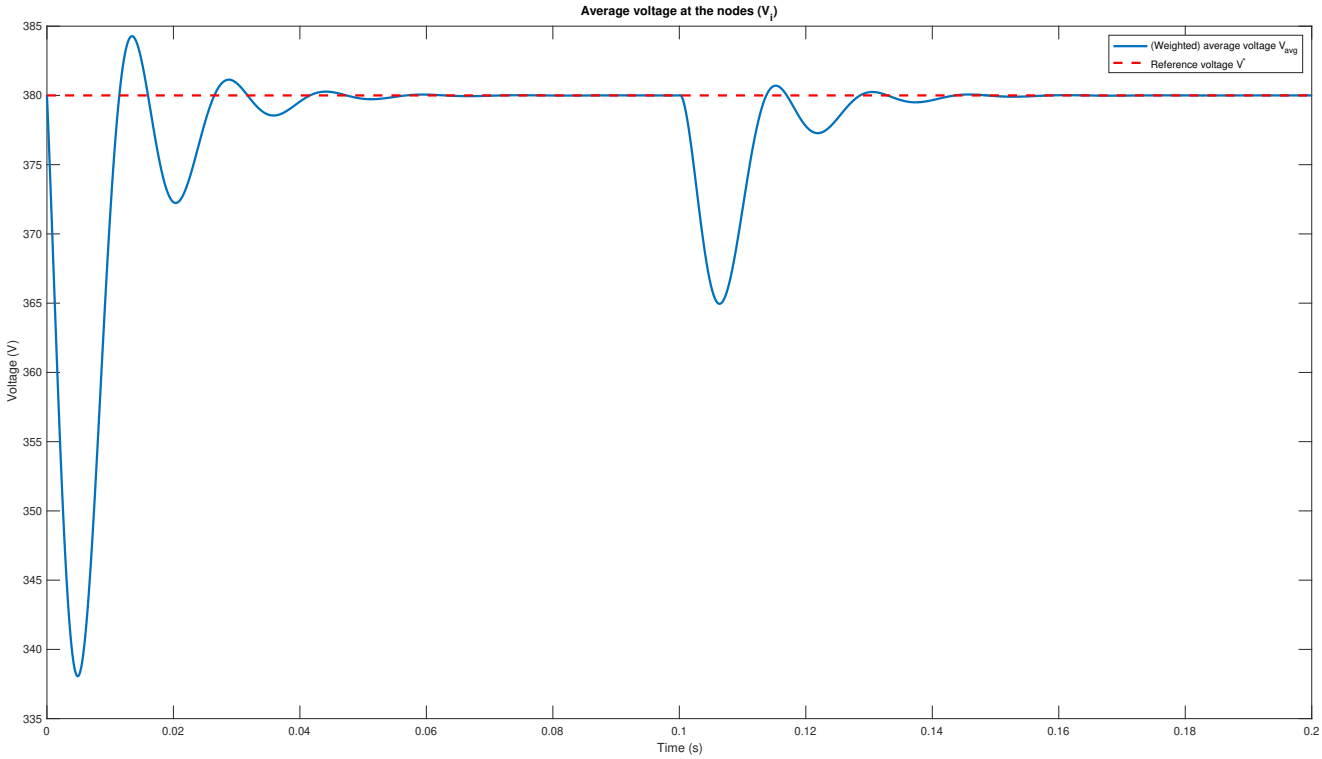

Figure 6.10: Weighted average voltage of all the nodes in the network during failure of power line k_{41}

As shown in Figure 6.10, average voltage regulation is still achieved when power line k_{41} fails during operation. It is shown that the weighted average voltage of the nodes in the network converge to the reference voltage. However, compared to Figure 6.5, it is observed that convergence time is longer than the constant current demand variation occurs.

6.2.2 Failure of power line k_{12}

The second power line failure that is identified in the four node network, is the failure of power line k_{12}. Compared to the connection of node 1 and node 4, node 1 and node 2 are connected by both power line and a communication link. During failure of the power line or the communication link, the other connection still remains. Therefore, during failure of power line k_{12}, DGU 1 and DGU 2 keep communicating by communication link γ_{12}.
In Figure 6.11, power line k_{12} is marked in red.

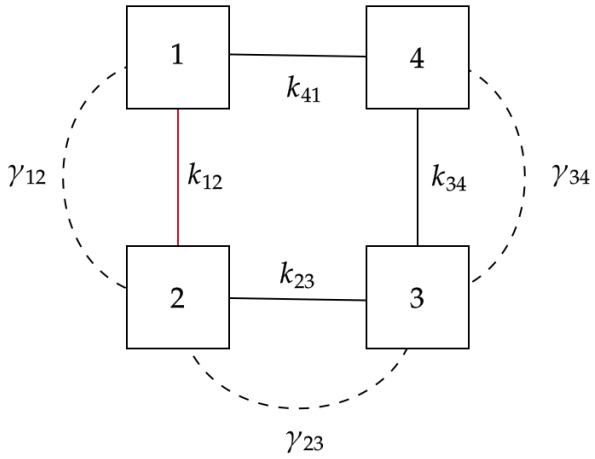

Figure 6.11: Failure of power line k_{12}

The power line failure is simulated at $t = 0.1s$, when the system is at steady state. Similar to the previous scenario, despite the network topology, the system parameters remain the same during failure of power line k_{12}.

The DGU parameters and line parameter can be found in Table 6.8 and Table 6.9 respectively.

Table 6.8: DGU parameters during failure of power line k_{41}

DGU		1	2	3	4
L_{ti}	(mH)	1.8	2.0	3.0	2.2
C_{ti}	(mF)	2.2	1.9	2.5	1.7
W_i	$(-)$	0.4^{-1}	0.2^{-1}	0.15^{-1}	0.25^{-1}
$V_i^\star$	(V)	380.0	380.0	380.0	380.0
$I_{li}^*(0)$	(A)	30.0	15.0	30.0	26.0
$Y_{li}^*(0)$	(mS)	3.08	3.08	3.08	3.08
$P_{li}^*(0)$	(kW)	7.8	7.8	7.8	7.8

Table 6.9: Line parameters after failure of power line k_{12}

Line		{2,3}	{3,4}	{4,1}
R_{ij}	(mΩ)	50	80	60
L_{ij}	(μH)	2.3	2.0	1.8

Equivalently to the scenario of power line k_{41} failure, the power flow across edge k_{12} at $t = 0.1s$ decreases to zero when the power line fails, as shown in Figure 6.12.

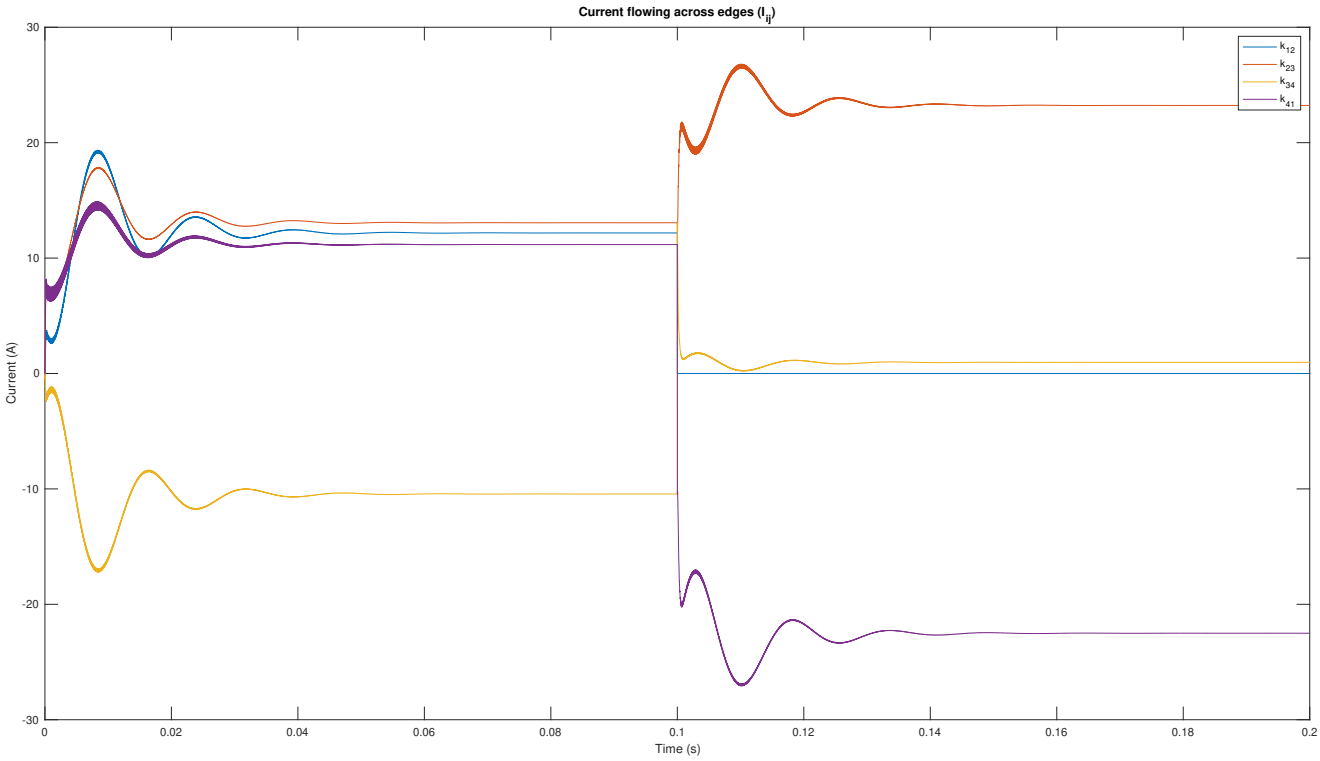

Figure 6.12: Current flow across edges during failure of power line k_{12}

Again, the current flow across the other power lines changes, which implies that the current takes a "new route" to meet the load demands of all the loads in the network. Negative current flow means that the current flows in the reversed direction than initialised by the incidence matrix. Clearly, the failure of power line k_{12} increases the peak load of the power lines which might cause stability issues if the current flow across the power lines exceeds the power line maximum current capacity.

Power sharing

In order to determine if power sharing is still achieved, Figure 6.13 shows a plot of the result of "unweighted" power at the nodes. "Unweighted" power means that the power at each node is compensated for its assigned weight.

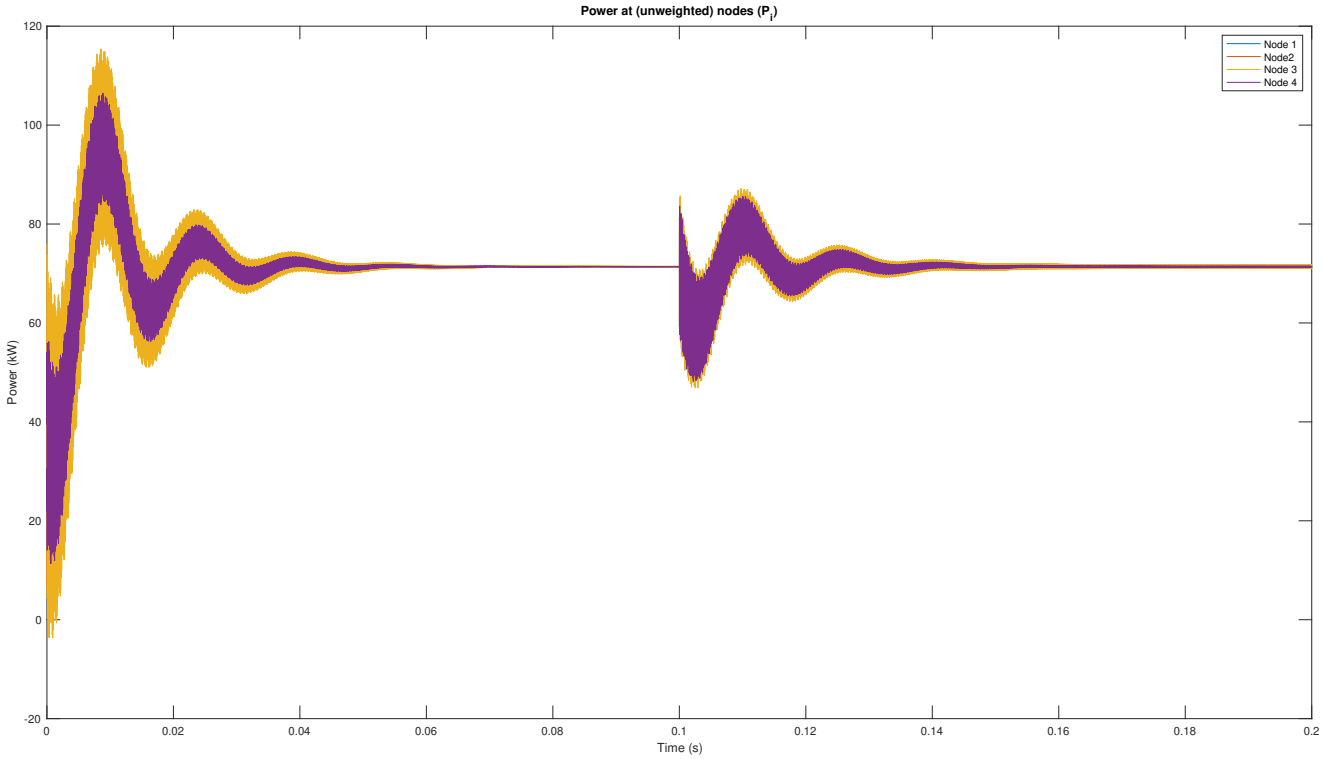

Figure 6.13: Fair power sharing among nodes during failure of power line k_{12}

Figure 6.13 shows that power sharing is achieved if power line k_{12} fails during operation of the microgrid. As expected, the control scheme requires time to find a new power consensus value. Despite the power line topology, the parameters remain identical. Therefore, the unweighted power at the nodes converge to the same power consensus value P^* as prior to the power line failure.

Average voltage regulation

In order to determine if weighted average voltage regulation is still achieved, Figure 6.14 plots the result of the weighted average voltage of node $i = 1 \dots 4$ and the reference voltage V^* which is preset by the operator.

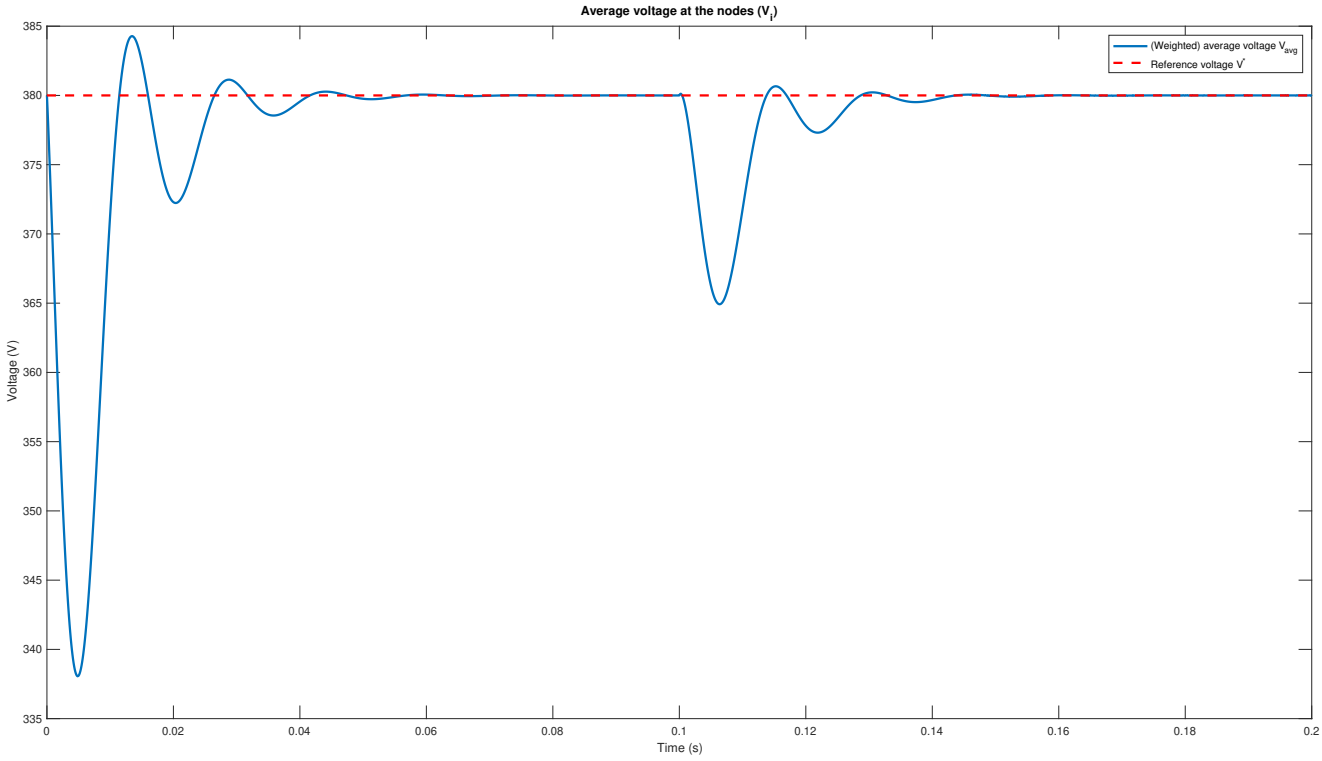

Figure 6.14: Weighted average voltage of all the nodes in the network during failure of power line k_{12}

As shown in Figure 6.14, average voltage regulation is still achieved when power line k_{12} fails during operation. It is shown that the weighted average voltage of the nodes in the network converge to the reference voltage. Compared to Figure 6.10, it is observed that convergences times, undershoot- and overshoot values are approaching each other.

6.2.3 Failure of power line k_{41} and k_{12} − isolation of node 1

In the next scenario, failure power line k_{41} and k_{12} are simulated simultaneously. In this event, DGU 1 becomes isolated, since it is not connected to the other DGUs in the network by power lines. However, DGU 1 keeps communicating with DGU 2 through communication link γ_{12}.
In Figure 6.15, the power lines that fails are marked in red.

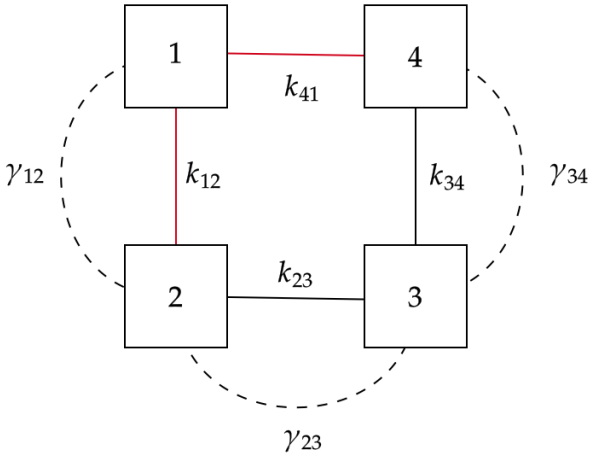

Figure 6.15: Failure of power line k_{41} and k_{12}, which results in isolation of DGU 1

The failure of two power line is simulated simultaneously at $t = 0.1s$, when the system is at steady state. As similar to the previous scenario, despite the network topology, the system parameters remain the same during failure of the power lines.
It is important to mention that if a DGU is not connected to any other DGU in a network by power lines, it is impossible to share generated power with other DGUs in a network.

The DGU parameters and line parameter can be found in Table 6.8 and Table 6.11 respectively.

Table 6.10: DGU parameters during failure of power line k_{41} and k_{12}

DGU		1	2	3	4
L_{ti}	(mH)	1.8	2.0	3.0	2.2
C_{ti}	(mF)	2.2	1.9	2.5	1.7
W_i	(−)	0.4^{-1}	0.2^{-1}	0.15^{-1}	0.25^{-1}
$V_i^\star$	(V)	380.0	380.0	380.0	380.0
$I_{li}^*(0)$	(A)	30.0	15.0	30.0	26.0
$Y_{li}^*(0)$	(mS)	3.08	3.08	3.08	3.08
$P_{li}^*(0)$	(kW)	7.8	7.8	7.8	7.8

Table 6.11: Line parameters after failure of power line k_{41} and k_{12}

Line		{2,3}	{3,4}
R_{ij}	(mΩ)	50	80
L_{ij}	(μH)	2.3	2.0

Power sharing and average voltage regulation

Figure 6.16 shows a plot of the result of the voltage at PCC of nodes $1, \ldots, 4$. The graph shows that at time when the two power lines fail simultaneously, the voltage at the isolated node (node 1) increases to high values. As shown in the figure, the voltage at node 1 increases to over 550V in a time span of just 0.1 seconds.
On the other hand, the voltages at PCC of node 1,2 and 3 decrease after failure of power line k_{41} and k_{12}. It is noticed that the decrease of voltage at node 1,2 and 3 follow a similar trend as the increase of voltage at node 1.

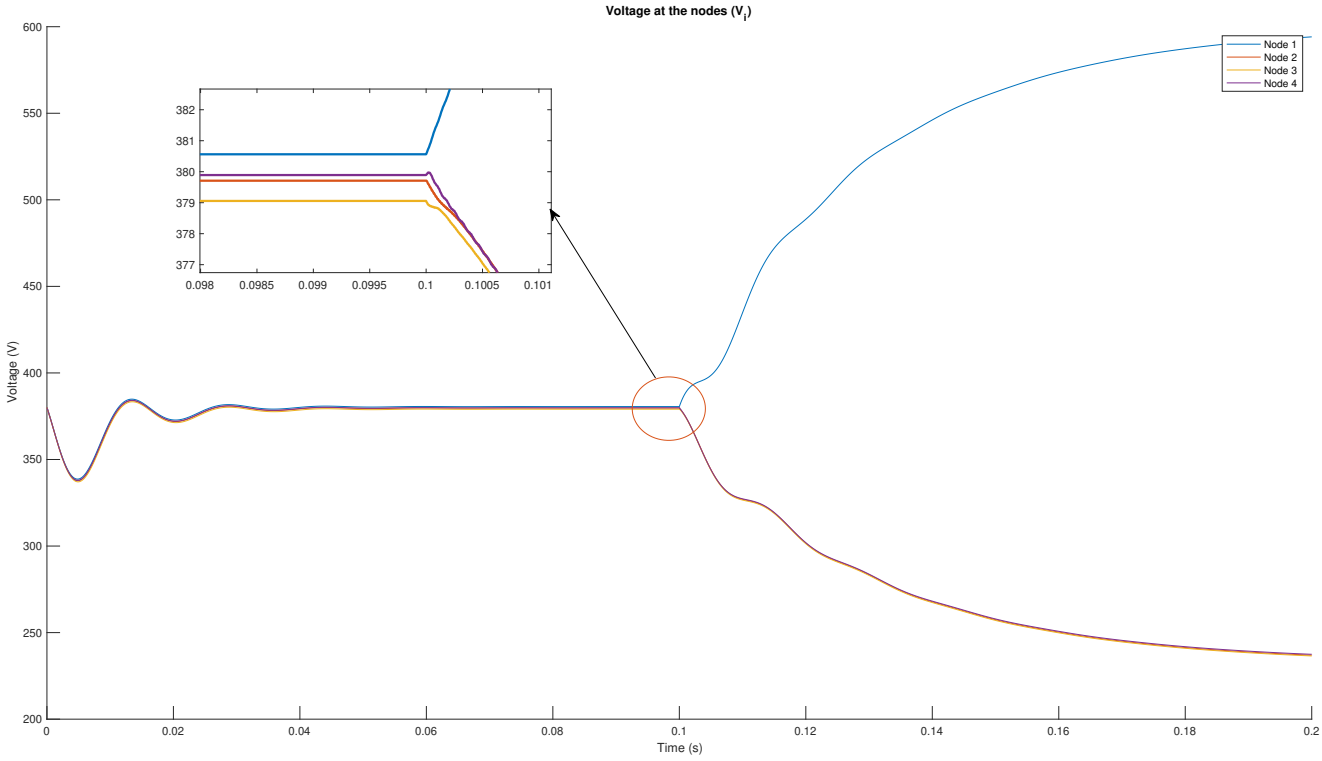

Figure 6.16: Voltage at PCC of DGU $1, \ldots, 4$

At $t \geq 0.1s$ DGU 1 is not connected to any other DGU in the network by power lines. Therefore, it is physically impossible to share power with the other DGUs. In fact, DGU 1 is only able to generate power to meet the demand of its own loads. However, DGU 1 remains to communicate its generated power and controller state θ, the neighbouring DGUs are not aware that power lines of DGU 1 are disconnected and DGU is isolated. Therefore, the other DGUs in the network "think" that DGU 1 is capable of share its generated power. As a result, DGU 2, 3 and 4 adjust their power generation according to the power generation of DGU 1.

Although Figure 6.17 shows power sharing among the four DGUs in the network, power sharing is only theoretically achieved.

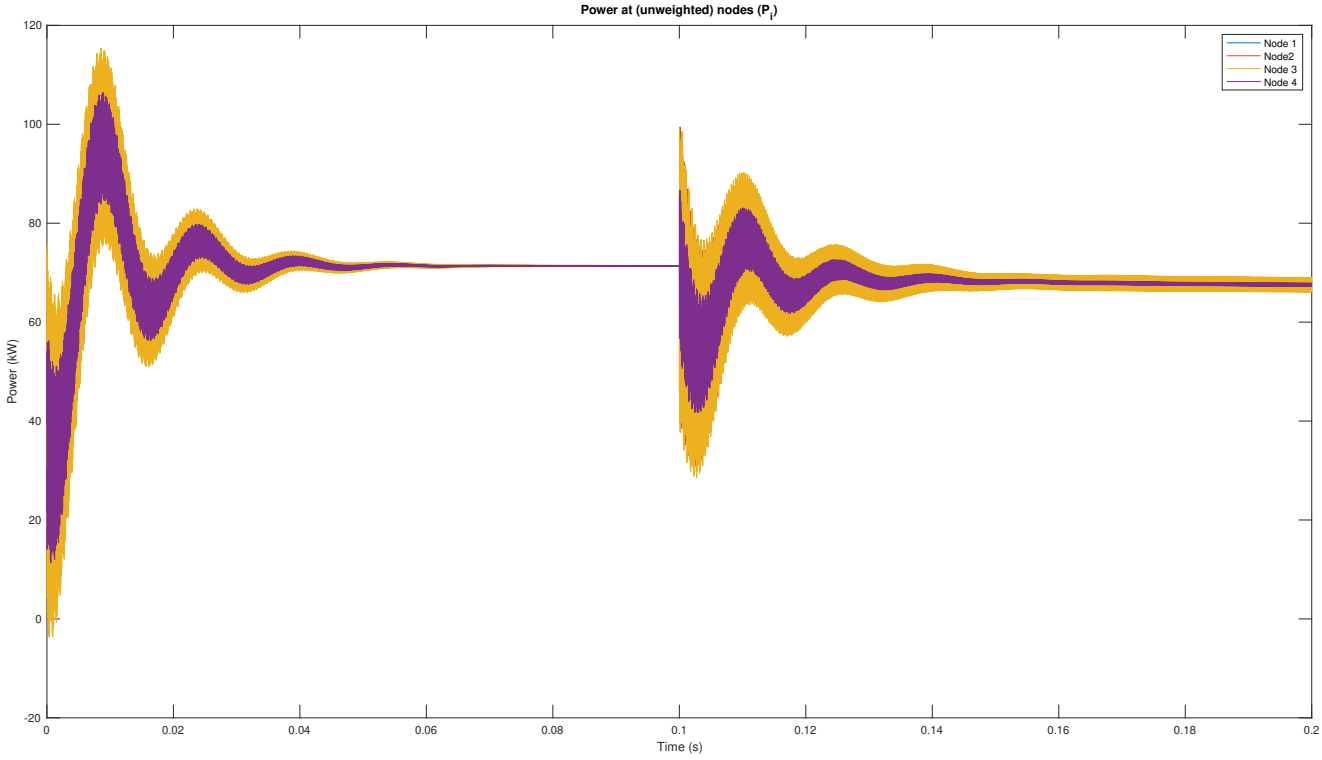

Figure 6.17: Fair power sharing among DGUs during isolation of DGU 1

However, to determine if weighted average voltage regulation is achieved, in Figure 6.18 the results are plotted of the weighted average of the four DGUs in the network together with the reference voltage V^*, which is preset to 380V.

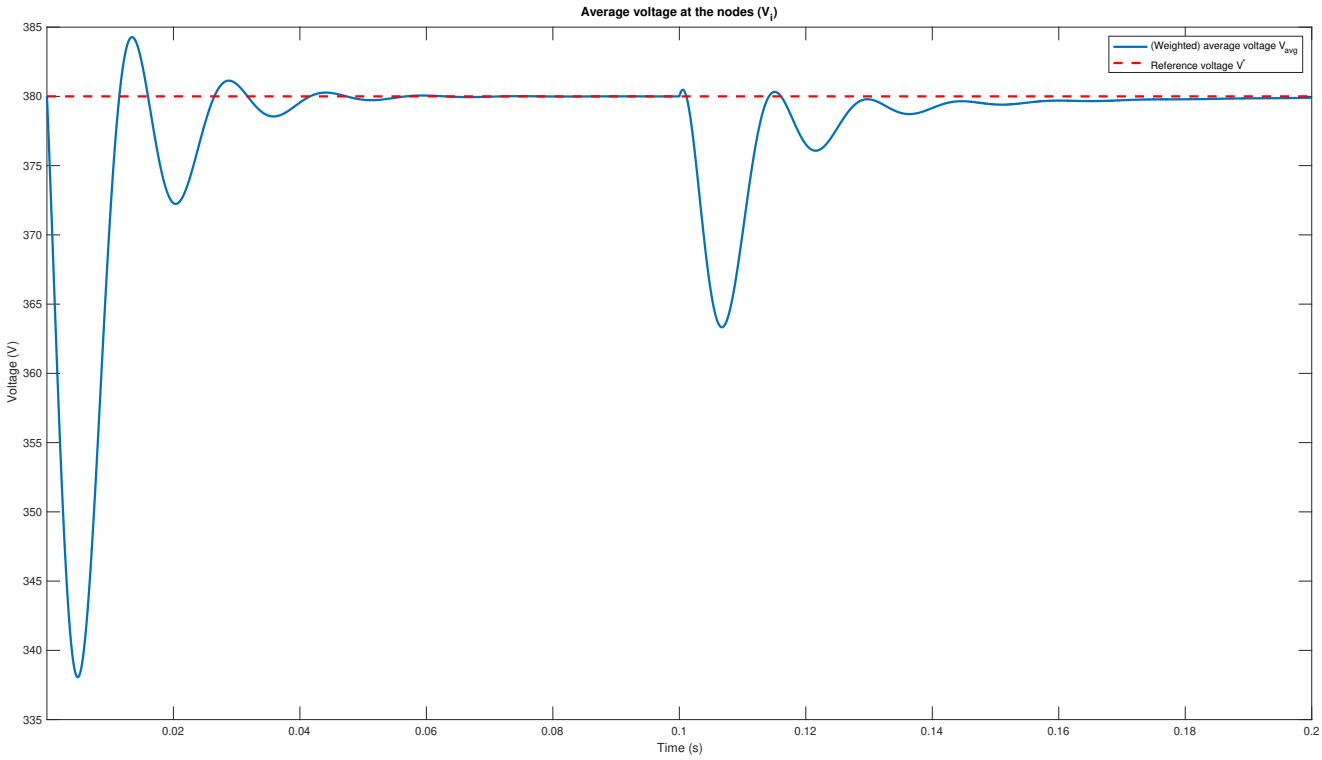

Figure 6.18: Weighted average voltage of all the nodes in the network

Figure 6.18 shows that the weighted average voltages of the nodes is equal to the reference value at steady state ($\overline{V} = V^*$). Besides, it is observed that it takes longer to reach a consensus value after the isolation of node 1 and compared to the failure of one power line.

6.3 Communication link failure

In this scenario, failure of communication link γ_{12} is simulated. It is chosen to simulate the failure of this communication line, because if the single communication link that is connected to DGU 1 fails, this DGU is communicative isolated from the rest of the network. In contradiction to the previous scenarios, no power line failure occurs.
In Figure 6.19, the communication link that fails is marked in red.

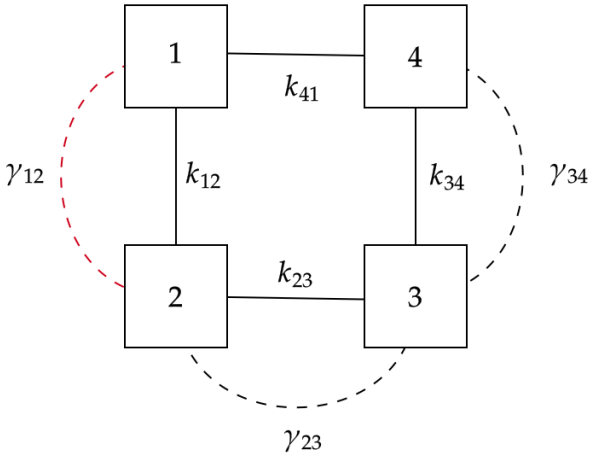

Figure 6.19: Failure of communication link γ_{12}

The failure of the communication link is simulated at $t = 0.125s$, when the system is at steady state. To reach steady state after failure of communication linke γ_{12}, the simulation runs for 5 seconds. As similar to the previous scenario, despite the network topology, the system parameters remain the same during failure of the communication line and can be found in Table 6.4 andTable 6.5.

Power sharing

In order to determine if power sharing is achieved among node $1, \ldots, 4$ if node 1 does not communicate with other nodes, the result of "unweighted" power at the nodes is plotted in Figure 6.20. "Unweighted" power means that the power at each node is compensated for its assigned weight.

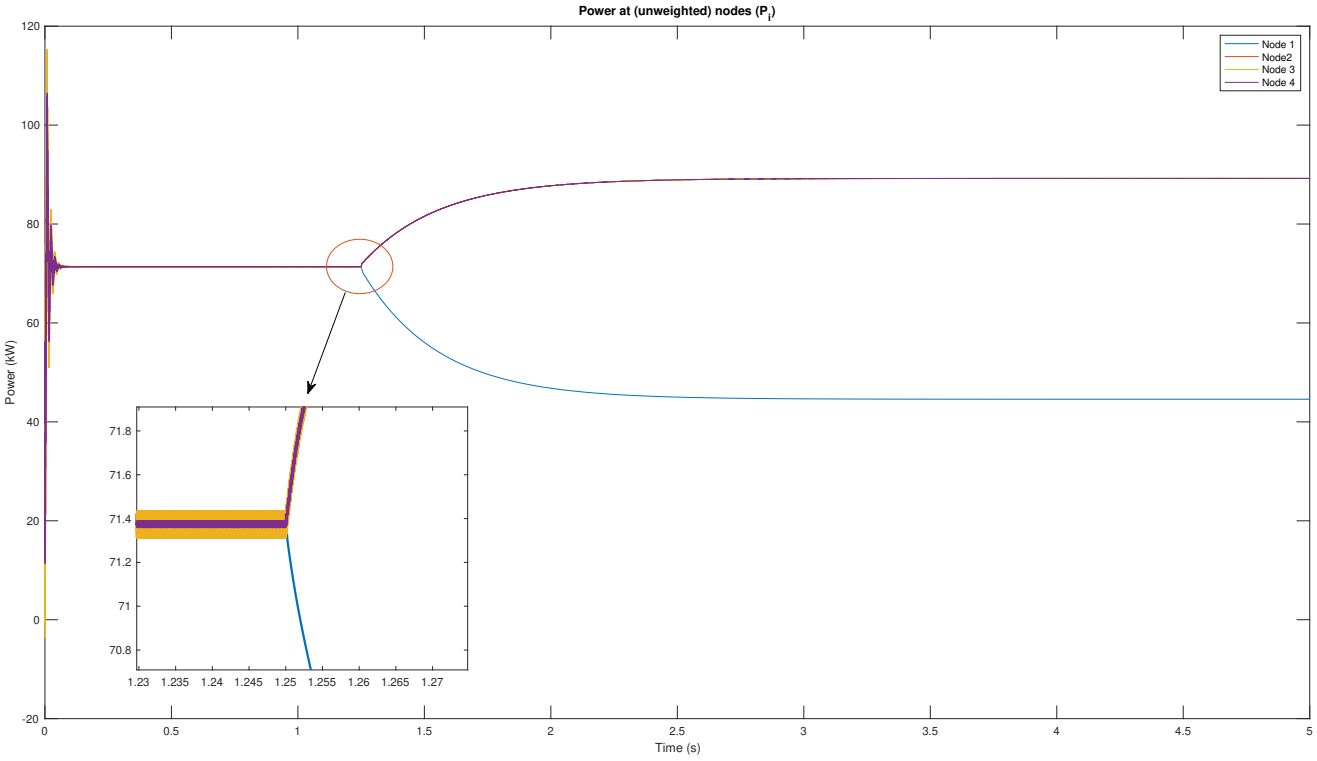

Figure 6.20: Fair power sharing among all DGUs during failure of communication link γ_{12}

Figure 6.13 shows that power sharing is among all the four DGUs is not achieved after communication link γ_{12} fails. It is observed that DGU 1 (blue line), which is not able to communicate with other nodes, is not able to fairly share power with the other DGUs in the network that are able to communicate. However, the unweighted power reaches a steady state value for every DGUs in the microgrid.
The underlying rationale is that the current applied to the terminals ($\dot{I}_l$) is based on the difference between the control input (u) and the voltage at PCC (V) of the corresponding DGU as shown in Equation 6.1:

$$L_t \dot{I}_t = -V + u \tag{6.1}$$

However, the control input u applies current to the terminals according to the generated power of the neighbouring DGUs that are exchanged via communication network ($\mathcal{L}^{com}\theta$) as shown in Equation 6.2:

$$u = -K(I_t - \phi) + W\mathcal{L}^{com}\theta + V^* \tag{6.2}$$

Which implies that the current applied to the terminals is not able to consider the power generated at DGU 1 as shown in Figure 6.21, which is a plot of the current measured at the converter of DGU $1, \ldots, 4$. This figure shows that the behaviour of the current over time at DGU 2, 3 and 4 show parallelity, because the power generated at DGU 2, 3 and 4 are exchanged over the communication network.

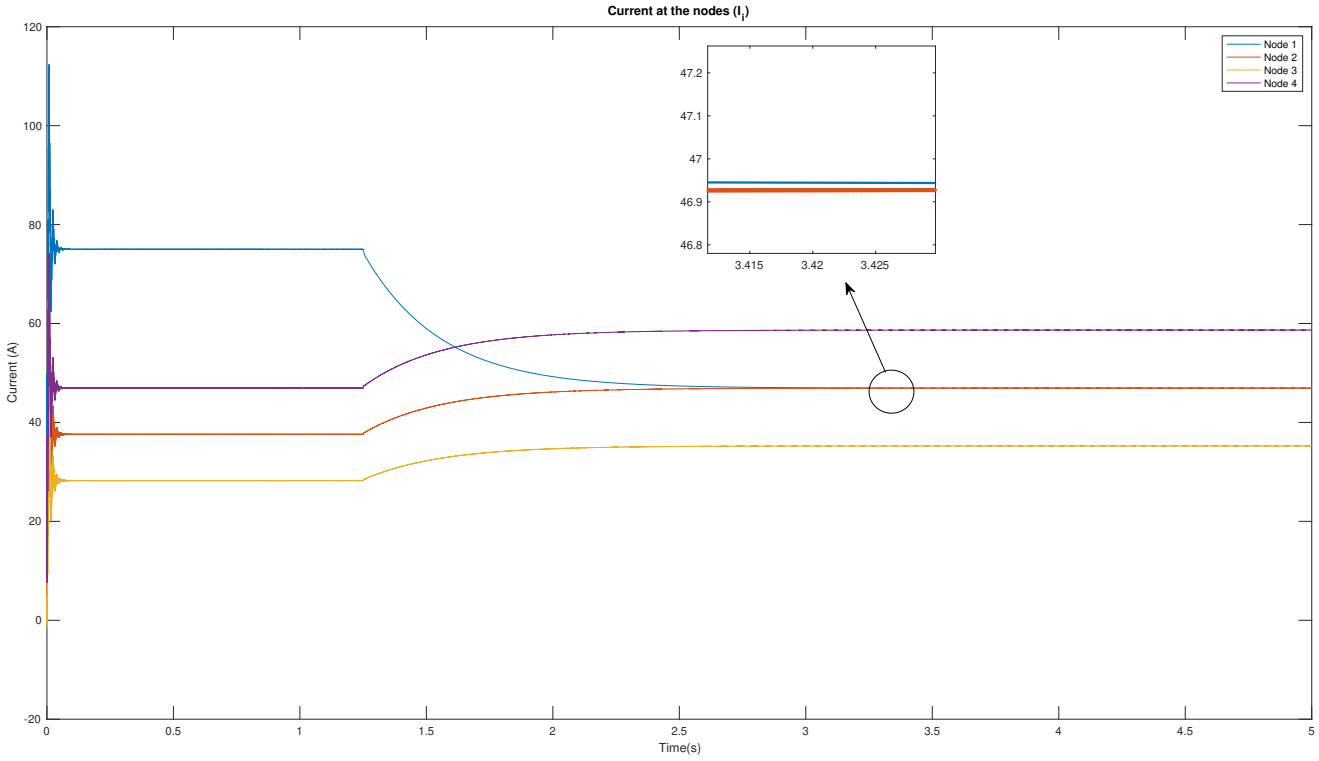

Figure 6.21: Measured current (I_t) at the converter of DGU $i = 1, \ldots, 4$ in the network during failure of communication link γ_{12}

From Figure 6.21, It is observed that the current at DGU $i = 1, \ldots, 4$ reach steady state values. Remarkably, the measured current at DGU 1 approaches the current measured at DGU 2 at steady state. Besides, the generated current dynamics of DGU $i = 2, \ldots, 4$ show a linear pattern, because these three nodes continue communicating their injected power (i.e. generated current and voltage at PCC).

Average voltage regulation

In order to determine if weighted average voltage regulation is achieved, Figure 6.10 plots the result of the weighted average voltage of node $i = 1 \dots 4$ and the reference voltage V^* which is preset by the operator at 380V.

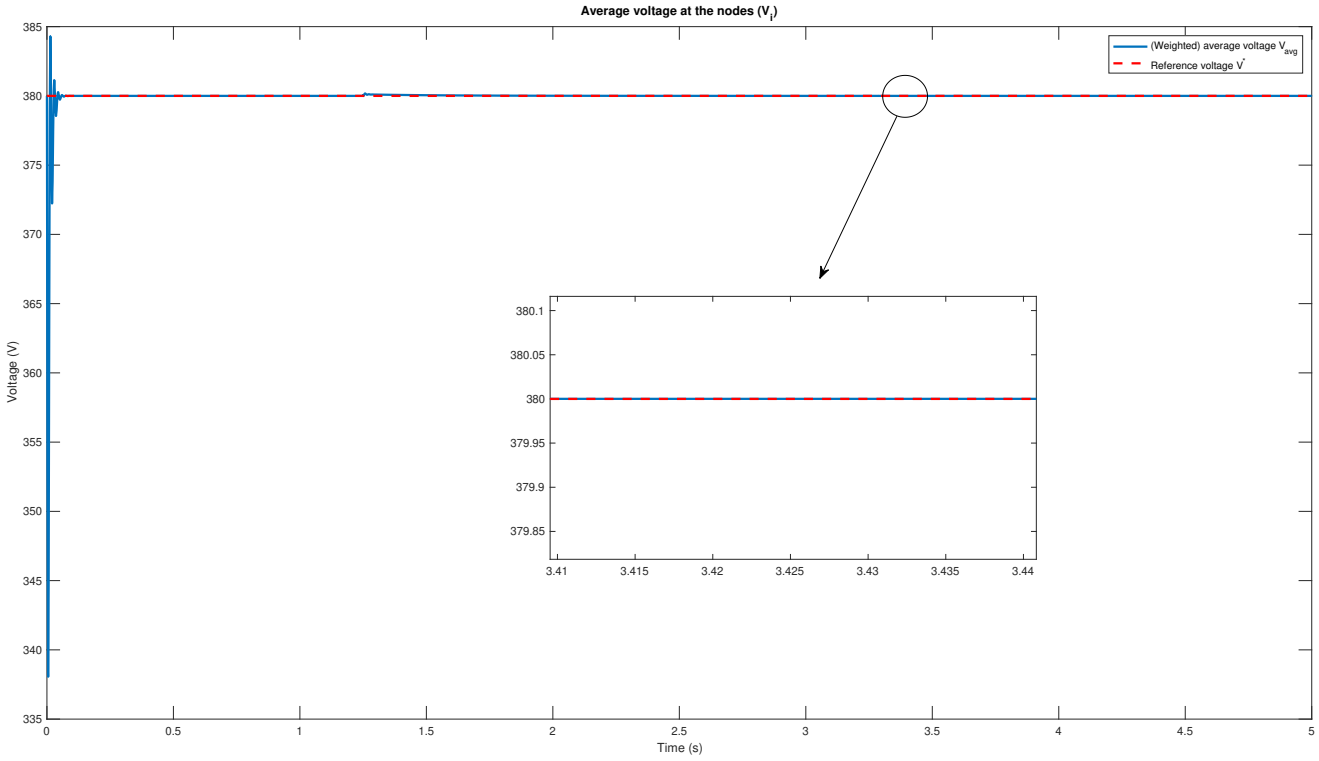

Figure 6.22: Weighted average voltage of all the nodes in the network during failure of communication line γ_{12}

As shown in Figure 6.22, average voltage regulation is when communication line γ_{12} fails during operation. It is shown that the weighted average voltage of the nodes in the network converge to the reference voltage.
The rationale that power sharing is not achieved and weighted voltage regulation is achieved when a communication link fails, is reduced from the weigthed average voltage regulation objective function Equation 5.15.

To recall, at steady state $\overline{\phi} = \overline{I_t}$. Then, the expression that describe the generated current at steady state ($\overline{I_t}$) (Equation 5.13a) results in:

$$\mathbf{0} = -\overline{V} + W\mathcal{L}^{com}\overline{\theta} + V^{\star} \tag{6.3}$$

Multiply both sides of Equation 6.3 with $\mathbf{1}^{\top}W^{-1}$ and after rewriting, Equation 6.3 shows that voltage at PCC of the DGUs converge to the desired reference voltage at steady state.

$$\mathbf{1}^{\top}W^{-1}(\overline{V} - V^*) = 0 \tag{6.4}$$

Equation 6.4 shows that to achieve average voltage regulation, the control scheme is not dependent of the communication network. Therefore, during failure of communication link γ_{12}, weighted average voltage regulation is achieved.

6.4 Plug-and-play

In this series of scenarios, the performance of the control scheme is investigated on the feature of plug-and-play in microgrids. One of the main important issues in microgrids is plug- and-play (PnP) operation of distributed generations units due to inherently discontinuous nature of renewable energy sources (Sadabadi et al., 2017). The concept of "plug-and-play" defines that the system is able to configure and integrate a component into the system by simply plugging it in. An automatic process determines the nature of the connected component to properly configure and operate (Nguyen et al., 2018).

In order to investigate the performance of the control scheme on this concept, the following two scenarios are simulated:

1. Plug in of DGU 5
   In this scenario, DGU 5 is plugged into the network of four DGUs that is schematic represented in Figure 6.6. DGU 5 is plugged connected to DGU 4 by a power line k_{45} and a communication link γ_{45}
2. plug out of DGU 4
   In this scenario, DGU 4 is plugged out of the four DGU network that is schematic represented in Figure 6.6. After DGU 4 is plugged out of the network, a three DGU network remain

The performance of the control scheme during the scenarios of plug in and plug out of DGUs, is investigated regarding power sharing and average voltage control regulation.

6.4.1 Plug in DGU 5

In this scenario, the plug in DGU 5 is simulated, including power line k_{45} and communication link γ_{45}. It is arbitrarily chosen to connect DGU 5 with DGU 4, since connecting DGU 5 to any other DGU in the network will provide identical results.
In Figure 6.23, the DGU, power line and communication link that are added are marked in green.

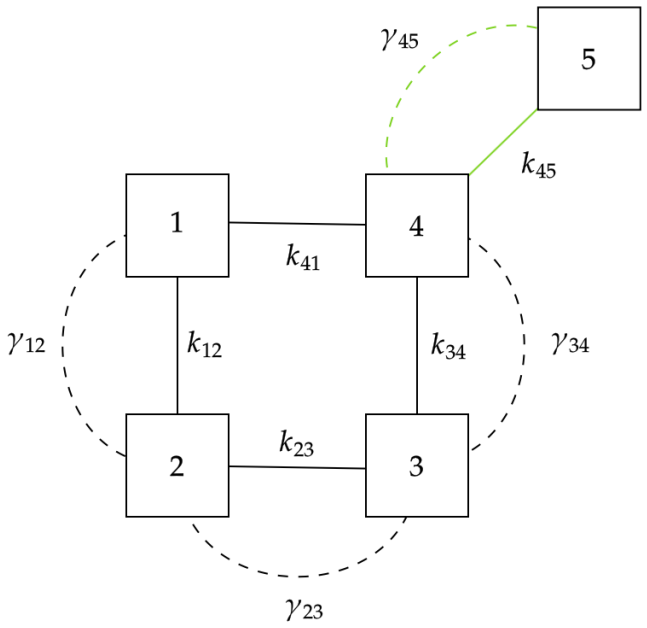

Figure 6.23: Plug in DGU 5

The plug in of DGU 5 simulated at $t = 0.1s$, when the system is at steady state. Before DGU 5 is plugged it, it is assumed, that the DGU is turned off. This results in the updated microgrid parameter values, where the parameters required to plug in DGU 5 are added.

The DGU parameters and line parameter can be found in Table 6.12 and Table 6.13

Table 6.12: DGU parameters when DGU 5 is plugged in.

DGU		1	2	3	4	5
L_{ti}	(mH)	1.8	2.0	3.0	2.2	2.6
C_{ti}	(mF)	2.2	1.9	2.5	1.7	2.1
W_i	$(-)$	0.4^{-1}	0.2^{-1}	0.15^{-1}	0.25^{-1}	0.3^{-1}
$V_i^\star$	(V)	380.0	380.0	380.0	380.0	380.0
$I_{li}^*(0)$	(A)	30.0	15.0	30.0	26.0	28.0
$Y_{li}^*(0)$	(mS)	3.08	3.08	3.08	3.08	3.08
$P_{li}^*(0)$	(kW)	7.8	7.8	7.8	7.8	7.8

Table 6.13: Line parameters after DGU 5 is plugged in

Line		{1,2}	{2,3}	{3,4}	{4,1}	{4,5}
R_{ij}	(mΩ)	70	50	80	60	70
L_{ij}	(μH)	2.1	2.3	2.0	1.8	1.9

Power sharing

In order to determine if power sharing is achieved between all the DGUs in the network, Figure 6.24 plots the results of unweighted power at the nodes. "Unweighted" power means that the power at each node is compensated for its assigned weight.

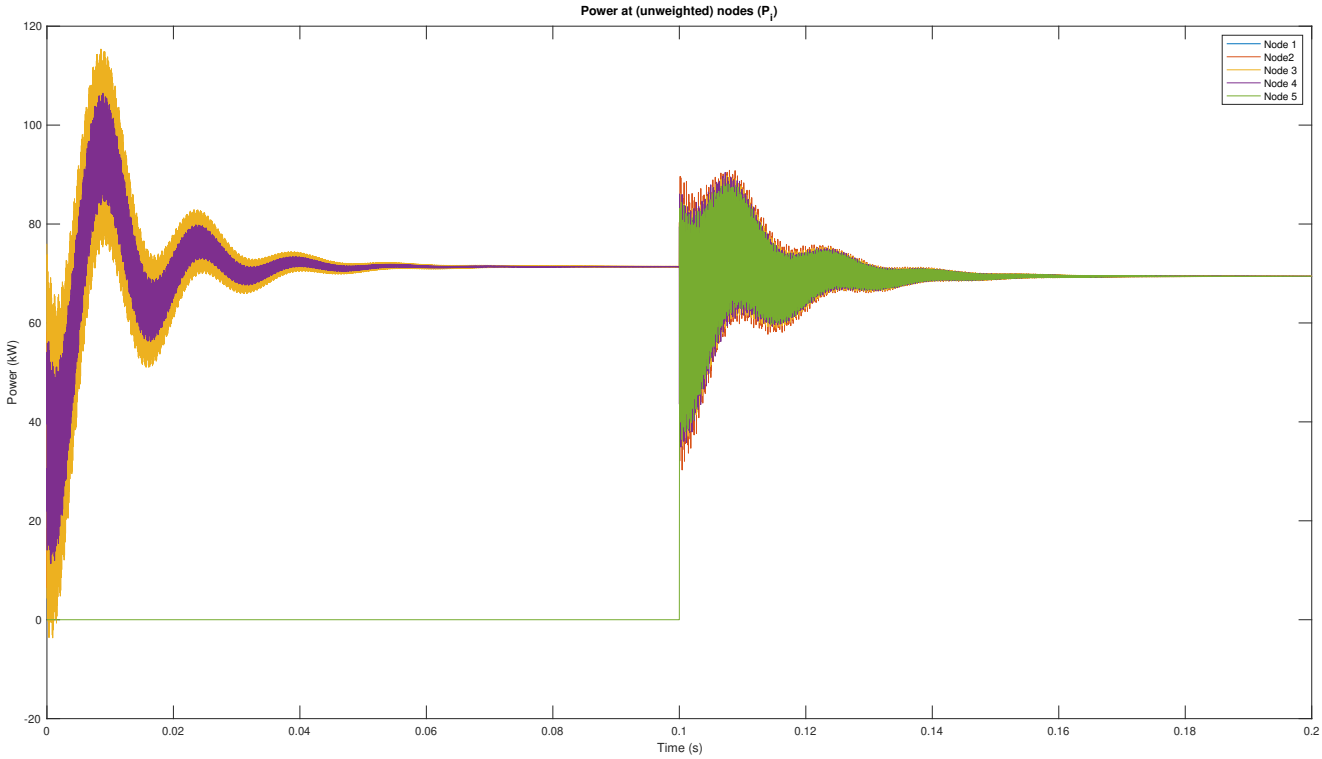

Figure 6.24: Fair power sharing among all DGUs during plug in of DGU 5

Figure 6.24 shows that power sharing is achieved among the DGUs in the network, even when a DGU is plugged in. The graph shows that the power at DGU 5 is zero during during the first time span, as it is plugged at $t = 0.1$. Until $t = 0.1$, DGU 5 is assumed to be turned off, which result in zero power generation. As expected, the control scheme requires time to find a new power consensus value. Depending on the weight that is assigned to the DGU, the new power consensus value differs from the power consensus value of the network topology prior to the plug in of DGU 5.

Average voltage regulation

In order to determine if weighted average voltage regulation is still achieved, Figure 6.25 plots the result of the weighted average voltage of DGU $i = 1, \ldots, 4$ for $0 \leq t < 0.1s$ and the weighted average voltage of DGU $i = 1, \ldots, 5$ for $0.1 \leq t \leq 0.2s$ the reference voltage V^* which is preset by the operator.

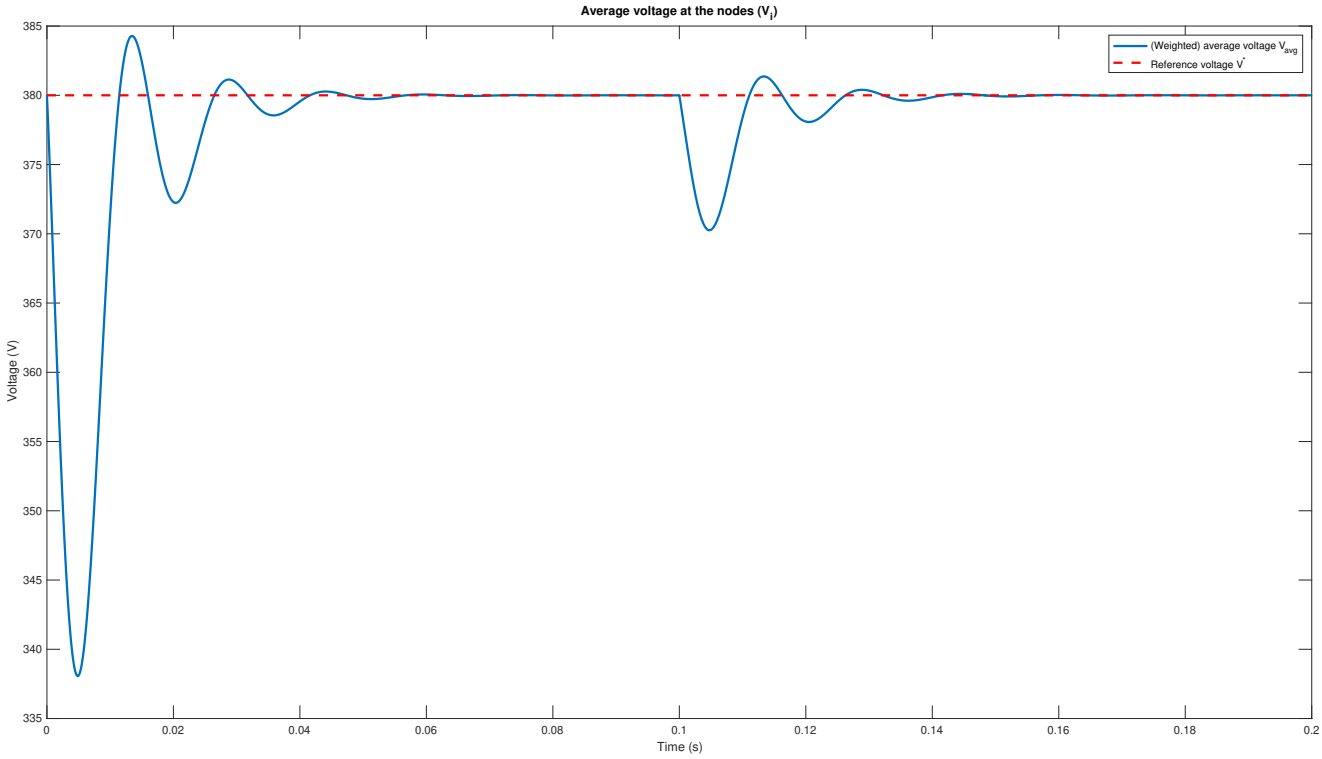

Figure 6.25: Weighted average voltage of connected nodes in the network

As shown in Figure 6.25, average voltage regulation is still achieved if DGU is plugged in during operation. It is shown that the weighted average voltage of the nodes in the network converge to the reference voltage. At steady state $\overline{V} = V^*$.

6.4.2 Plug out DGU 4

In this scenario, the plug out DGU 4 is simulated, including power lines k_{41}, k_{34} and communication link γ_{34}. DGUs are plugged out of the microgrid for various reasons (e.g. maintenance purposes). It is chosen to plug out DGU 4, since this DGU is connect identical connected to two nodes. DGU 4 is connected to DGU 3 by a power line and a communication link, while it is connected to DGU 1 by only a power line.
In Figure 6.26, the network topology of the network after plug out DGU 4 is schematic represented.

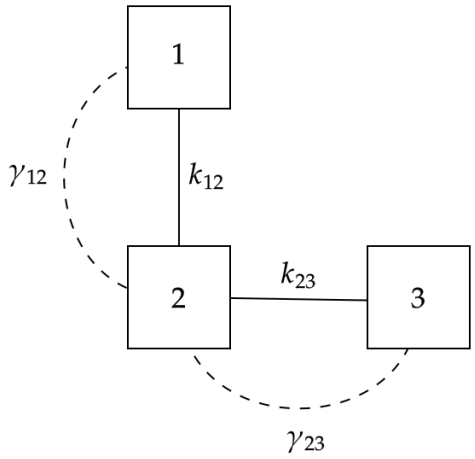

Figure 6.26: Plug out DGU 4

The plug out of DGU 4 simulated at $t = 0.1s$, when the system is at steady state. When DGU 4 is plugged out, it is assumed, that the DGU is turned off. As similar to the previous scenarios, despite the network topology, the system parameters remain the same during plug out of DGU 4.

The DGU parameters and line parameter can be found in Table 6.14 and Table 6.15

Table 6.14: DGU parameters after DGU 4 is plugged out

DGU		1	2	3
L_{ti}	(mH)	1.8	2.0	3.0
C_{ti}	(mF)	2.2	1.9	2.5
W_i	(−)	0.4^{-1}	0.2^{-1}	0.15^{-1}
$V_i^\star$	(V)	380.0	380.0	380.0
$I_{li}^*(0)$	(A)	30.0	15.0	30.0
$Y_{li}^*(0)$	(mS)	3.08	3.08	3.08
$P_{li}^*(0)$	(kW)	7.8	7.8	7.8

Table 6.15: Line parameters after DGU 4 is plugged out

Line		{1,2}	{2,3}
R_{ij}	(mΩ)	70	50
L_{ij}	(μH)	2.1	2.3

Power sharing

In order to determine if power sharing is achieved between all the DGUs in the network, Figure 6.27 plots the results of unweighted power at the nodes. "Unweighted" power means that the power at each node is compensated for its assigned weight.

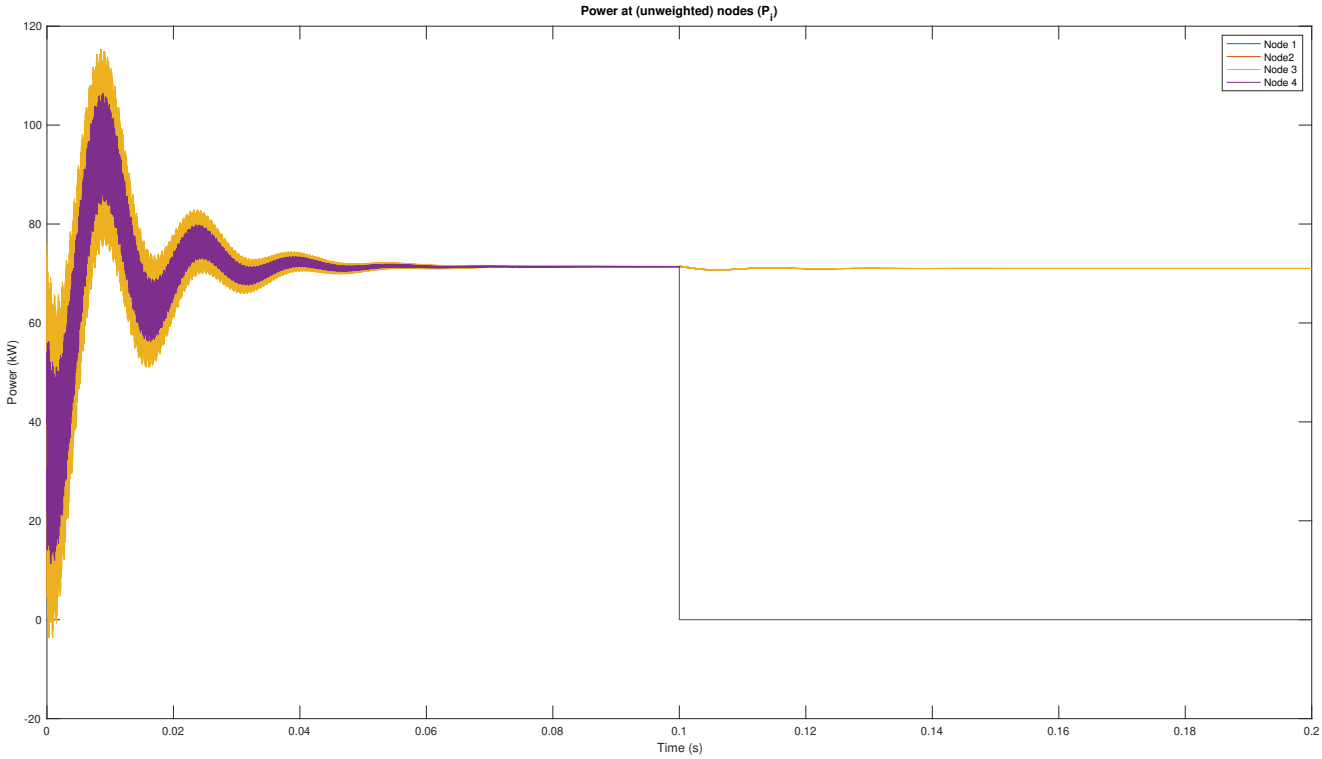

Figure 6.27: Fair power sharing among all DGUs during plug in of DGU 5

Figure 6.24 shows that power sharing is achieved among the DGUs in the network, even when an additional DGU is plugged in. The graph shows that the power at DGU 5 is zero during during the first time span, as it is plugged at $t = 0.1$. From $t = 0.1$, DGU 4 is assumed to be turned off, which result in zero power generation. Therefeore, the unweighted power at DGU 4 is zero for $t \geq 0.1s$. As expected, the control scheme requires time to find a new power consensus value. However, the convergence of the unweighted power to the consensus value is relatively fast, with minimum under- and overshoot.

Average voltage regulation

In order to determine if weighted average voltage regulation is still achieved, Figure 6.28 plots the result of the weighted average voltage of DGU $i = 1, \ldots, 4$ for $0 \leq t < 0.1s$ and the weighted average voltage of DGU $i = 1, \ldots, 3$ for $0.1 \leq t \leq 0.2s$, since DGU 4 is plugged out and assumed turned off for $t \geq 0.1s$. Furthermore, the reference voltage V^* is plotted, which is preset by the operator.

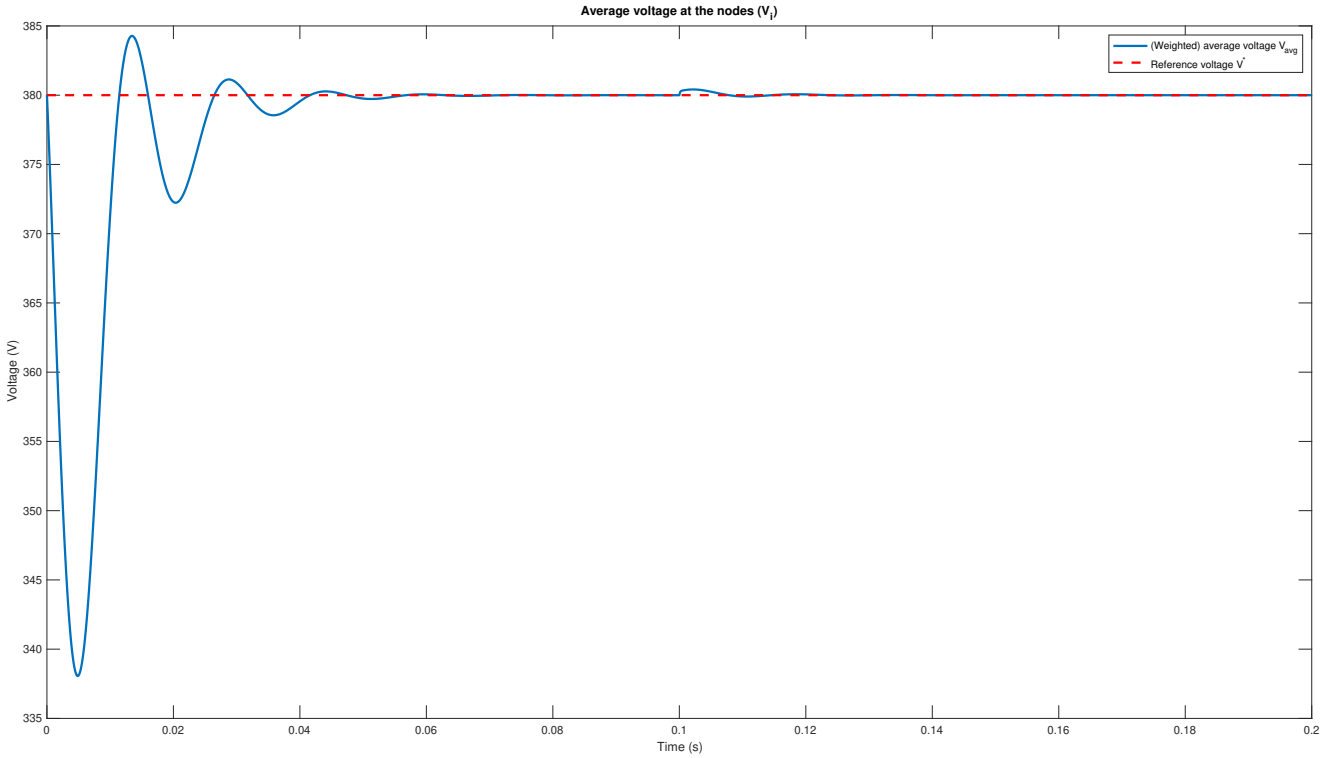

Figure 6.28: Weighted average voltage of connected nodes in the network

As shown in Figure 6.25, average voltage regulation is still achieved if DGU 4 is plugged out during operation. It is shown that the weighted average voltage of the nodes in the network converge to the reference voltage. At steady state $\overline{V} = V^*$.

6.5 Interpretation of results

Subsequent to the results of the extensive simulation of the control scheme to investigate its performance in critical scenarios, the results are interpreted in this section, which leads to important insights of the proposed controller regarding the design of microgrids.

Firstly, it can be concluded that the general performance of the control scheme is promising. The control scheme achieves fair power sharing among all the DGUs in a network and weighted average power sharing simultaneously in regular circumstances as shown by simulating the DC microgrid benchmark network. The proposed control scheme is robust to load demand variation, which is an ordinary circumstance during the operation of a DC microgrid.
Besides, it turned out that the control scheme is robust to power line failure in the network, since three different power line failure scenarios are simulated. During all three cases, fair power sharing and average voltage are theoretically achieved. When one power line fails in the system, the result shows that current flows through other power lines to meet load demands and achieve the control objectives, which is desired performance. However, during simultaneously failure of two power lines which results in isolation of a DGU, fair power sharing and average voltage regulation is theoretically achieved, but is impossible in reality. The reason behind this is that if a DGU is isolated by power lines, it is able to generate power to meet its own load demands, but unable to share its generated power. However, if the isolated DGU continue to communicate with other DGUs in the network, the controller will not notice that the DGU is isolated and not able to share its generated power.
This behaviour of the proposed control scheme is supported by the simulation of a communication link failure scenario. The result of the simulation shows that during the failure of a communication link, the controller is unable to achieve fair power sharing since to achieve this objective, the control scheme requires information about the power that is injected at neighbouring DGU. On the other hand, weighted average voltage regulation is achieved, since to achieve this objective, the control scheme does not rely on the state of the communication network. Besides, it is observed that the voltage at PCC of the DGU that is isolated, increases heavily. It is needless to say that this behaviour is undesirable since it can cause stability and safety issues.

The rationale behind this behaviour is found in the design of the control scheme. Namely, the microgrid is controlled in a distributed manner. This implies that no central controller is required and local controllers share information over a communication network. This concept is used to design the control scheme that is proposed in this research, where control states are shared via a communication network ($\mathcal{L}^{com}\theta$) as shown in Equation 5.12. The control input of a DGU is purely dependent on its own states and its neighbours states, which are exchanged by the communication network. Therefore power line failure, which results in isolation of a DGU or a cluster of DGUs, remains unnoticed and causes undesirable behaviour. Also, it is shown that every DGU must be connected to at least one other DGU. In the four DGU network that is used during simulation, some DGUs are connected in the communication network by a single communication link, which denotes that in this network, the control scheme is not immune to a single point of failure (SPOF).

The analysis of the simulation results leads to interesting insights regarding the design of a microgrid system. Although the performance of the control scheme is promising, some important aspects should be taken into consideration to ensure the safety and stability of a DC microgrid. It is advisable to obtain knowledge of the state of the power lines and communication links during all times. It is essential for the proper operation of the microgrid and its controllers that DGUs in a network are prevented for communicative isolation or power flow isolation. Isolation of DGUs in a microgrid network should directly be noticed (e.g. by sensors) to prevent power outages in the network. If a DGU is isolated by power line failure, the DGU must be plugged out of the network, to disconnect communication between the isolated DGU and the rest of the network. Similarly, if a DGu is communicatively isolated, it should stop generating power to prevent undesirable behaviour of the DGU in the microgrid network.

Chapter 7

Conclusion

In this chapter *research question 8* is addressed. This chapter determines the main conclusions of the thesis to add knowledge to existing literature. In this thesis, a distributed control scheme is proposed that achieves power sharing and average voltage regulation in DC microgrids to increase the stability and reliability of the power system. Besides, The performance of the proposed control scheme is investigated by simulation of critical scenarios that eventually happen in DC microgrids. Analysis of the results provides an appropriate performance indication and leads to interesting insights regarding the design of microgrids. Although the DC microgrid model that is used is fairly standard, the proposed control scheme shows some unique benefits over control schemes that are proposed in literature. which enhances the applicability of the proposed control scheme to control DC microgrids.

From the simulation study, it is concluded that the performance of the controller is promising. Under regular circumstances, fair power sharing and average voltage regulation are achieved simultaneously in various network topologies. Also, the proposed control scheme shows good performance in controlling a DC microgrid benchmark network.
As shown for two cases, the distributed control scheme is capable of handling power line failure in DC microgrids if the power line failure does not result in isolation of a DGU. Due to the property of DC microgrids that the communication network can differ from the power line network topology, three identical power line failures are identified in a four DGU microgrid. The results show that current flow via different power lines if a single power line fails to remain power sharing in the network. However, due to the design of the control scheme, to achieve power sharing, a DGU is dependent of its states, but also on a control state and the power that is injected at its neighbours. This information is shared via a communication network. Therefore, the control scheme only achieves fair power sharing and average voltage regulation if it receives the correct information from its neighbours. Due to this limitation, it is shown that power sharing is not achieved when failure of power line(s) results in the isolation of a DGU. A simulation is conducted where two power lines fail simultaneously and cause isolation of a DGU. The result shows that the controller's two objectives are not achieved. The reason is that isolated DGU keeps communicating its states to its neighbours when it is isolated. Therefore, the isolation of a DGU is not noticed, and the control scheme aims to share power between all the DGUs in the network, which is physically impossible.
Furthermore, the simulation of communication link failure endorses the vital role of the communication network in the control scheme to achieve power sharing. During the simulation of a communication link failure, a DGU became communicatively isolated, which means that it was not connected to any other DGU by a communication line. In this scenario, fair power sharing is not achieved. On the other hand, due to the design of the control scheme, the state of the communication network is does not affect the regulation of weighted average voltage. Therefore, if a DGU becomes communicatively isolated, weighted average voltage regulation will still be achieved.

The analysis of the simulation results leads to interesting insights regarding the design of microgrids. During the isolation of a DGU, the voltages level of that DGU increases to critical levels which decreases the safety and reliability of the power system. Therefore, the state of the power lines and communication lines should be monitored during all operation times to prevent the failure of power lines and communication links that result in the isolation of DGUs in the microgrid network. Sensors can be installed to measure the current flow across power lines to detect any failure of the power lines. If isolation of DGUs is directly noticed, corresponding DGUs can be plugged out of the network, or the power generation of the isolated DGU can be stopped to maintain power sharing and average voltage regulation in DC microgrids.

Chapter 8

Limitations and further research

The purpose of this chapter is to discuss the limitations of the current research, and put them into perspective for further research. It cannot be emphasized enough that the range of possibilities and approaches, in performing research on controlling and stabilizing dynamical networks as microgrids, is extraordinary. Many more research directions can be taken. This thesis provides the results of one strategy to control DC microgrids, but further research is necessary in order to implement this prospective grid in the future.

First of all, most of the parameters used in the current simulation studies, including load parameters, line parameters and DGU parameters, were adopted from other references such as Weitenberg (2018), Trip et al. (2018), De Persis et al. (2018). Due to the limited time span of the this study, validation of the large number of system parameters was not possible. In future research, this could be further investigated, by theoretical or empirical justification of the parameters and input data for specific microgrids.
Secondly, it would be interesting to extend the simulations by including scenarios, or apply the control algorithm to AC or hybrid microgrids, to investigate the performance of this control scheme in larger networks or AC microgrids. In literature, many current and power sharing methods are proposed (Han et al. (2017), Nasirian et al. (2014), Anand et al. (2012) and Zhao and Dörfler (2015)). Also, the voltage balancing problem is adressed in literature (Tucci et al. (2018) Nasirian et al. (2014)) An comparative evaluation of the control scheme performance that is proposed in this thesis with a control scheme proposed in literature would be a interesting for further research to obtain a better performance indication of the proposed control scheme.

Furthermore, the model can be further extended by including more dynamics. In the DC microgrid model that is developed in this research, the sources are considered to be controllable distributed generation units. The DGUs are constant power sources. However, renewable energy sources (e.g. solar, wind and tidal) are usually sources that are adopted in DC microgrid. These sources do not deliver constant power continuously, due to intermittent of nature (Shivashankar et al., 2016). Therefore, including power source dynamics would be an interesting extension which increase the complexity.
Besides, in the DC microgrid model that is considered in this work, a buck converter is used to step down voltage (while stepping up current) from its input (supply) to its output (load). Instead of a buck converter, buck-boost or boost converters can be considered, since boost converters are more desirable for PV sources. The dynamics of the DC microgrid model can be extended by including dynamics of the converter, which are nonlinear. (Cucuzzella et al., 2019c).

The last and most important limitation of this research is that a theoretical validation of the proposed control scheme is lacking. The conclusions regarding the performance of the control scheme are solely based on a simulation study. Although the control scheme shows promising performance during simulation, definite conclusions of the performance can not be given due to the lack of theoretical validation.
In order to validate the control scheme, the stability of the dynamical system must be proven. Stability is the most commonly studied property of invariant sets. Roughly speaking, an invariant set is called stable if trajectories starting close to it remain close to it, and unstable if they do not (Lestas, 2019). In this work, it is assumed that an equilibrium exist and that (I_t, V, I, T_θ, T_ϕ) always converge to a steady state solution ($\overline{I_t}$, $\overline{V}$, $\overline{I}$, $\overline{T_\theta}$, $\overline{T_\phi}$). Lyapunov theory is fundamental in systems theory (Kosaraju et al., 2018). By applying Lyapunov's direct method, stability of the dynamical system can be proven by finding a positive definite differential Lyapunov function, of which its derivative is semi-definite. If such a suitable Lyapunov candidate is found, the stability of the system dynamics can be proven.

Bibliography

Anand, S., Fernandes, B. G., and Guerrero, J. (2012). Distributed control to ensure proportional load sharing and improve voltage regulation in low-voltage dc microgrids. *IEEE transactions on power electronics*, 28(4):1900–1913.

Arif, M. S. B. and Hasan, M. A. (2018). Microgrid architecture, control, and operation. In *Hybrid-Renewable Energy Systems in Microgrids*, pages 23–37. Elsevier.

Beykverdi, M., Jalilvand, A., and Ehsan, M. (2017). Decentralized control of low-voltage islanded dc microgrid using power management strategies. *American Journal of Science, Engineering and Technology*, 1(2):27.

Cavanagh, K., Belk, J. A., and Turitsyn, K. (2017). Transient stability guarantees for ad hoc dc microgrids. *IEEE Control Systems Letters*, 2(1):139–144.

Conejo, A. J. and Baringo, L. (2018). *Power system operations*. Springer.

Cucuzzella, M., Incremona, G. P., and Ferrara, A. (2017). Decentralized sliding mode control of islanded ac microgrids with arbitrary topology. *IEEE Transactions on Industrial Electronics*, 64(8):6706–6713.

Cucuzzella, M., Kosaraju, K. C., and Scherpen, J. (2019a). Voltage control of dc networks: robustness for unknown zip-loads. *arXiv preprint arXiv:1907.09973*.

Cucuzzella, M., Kosaraju, K. C., and Scherpen, J. M. (2019b). Distributed passivity-based control of dc microgrids. In *2019 American Control Conference (ACC)*, pages 652–657. IEEE.

Cucuzzella, M., Lazzari, R., Kawano, Y., Kosaraju, K. C., and Scherpen, J. M. (2019c). Robust passivity-based control of boost converters in dc microgrids. In *2019 IEEE 58th Conference on Decision and Control (CDC)*, pages 8435–8440. IEEE.

Cucuzzella, M., Lazzari, R., Trip, S., Rosti, S., Sandroni, C., and Ferrara, A. (2018a). Sliding mode voltage control of boost converters in dc microgrids. *Control Engineering Practice*, 73:161–170.

Cucuzzella, M., Trip, S., De Persis, C., Cheng, X., Ferrara, A., and van der Schaft, A. (2018b). A robust consensus algorithm for current sharing and voltage regulation in dc microgrids. *IEEE Transactions on Control Systems Technology*, 27(4):1583–1595.

Datta, U., Kalam, A., and Shi, J. (2018). Hybrid pv–wind renewable energy sources for microgrid application: an overview. In *Hybrid-Renewable Energy Systems in Microgrids*, pages 1–22. Elsevier.

De Persis, C., Weitenberg, E. R., and Dörfler, F. (2018). A power consensus algorithm for dc microgrids. *Automatica*, 89:364–375.

de Souza, A. C. Z. and Castilla, M. (2019). *Microgrids Design and Implementation*. Springer.

DENA (2019). Energy Transition Trends 2019. https://www.dena.de/fileadmin/dena/

Dokumente/Themen_und_Projekte/Internationales/China/CREO/Energy_transition_trends_2019_engl.pdf.

Dorfler, F. and Bullo, F. (2012). Kron reduction of graphs with applications to electrical networks. *IEEE Transactions on Circuits and Systems I: Regular Papers*, 60(1):150–163.

EPA (2018a). Centralized Generation of Electricity and its Impacts on the Environment. https://www.epa.gov/energy/centralized-generation-electricity-and-its-impacts-environment.

EPA (2018b). Distributed Generation of Electricity and its Environmental Impacts. https://www.epa.gov/energy/distributed-generation-electricity-and-its-environmental-impacts.

Fei, G., Ren, K., Jun, C., and Tao, Y. (2019). Primary and secondary control in dc microgrids: a review. *Journal of Modern Power Systems and Clean Energy*, 7(2):227–242.

Guerrero, J. M., Chandorkar, M., Lee, T.-L., and Loh, P. C. (2012a). Advanced control architectures for intelligent microgrids—part i: Decentralized and hierarchical control. *IEEE Transactions on Industrial Electronics*, 60(4):1254–1262.

Guerrero, J. M., Loh, P. C., Lee, T.-L., and Chandorkar, M. (2012b). Advanced control architectures for intelligent microgrids—part ii: Power quality, energy storage, and ac/dc microgrids. *IEEE Transactions on Industrial Electronics*, 60(4):1263–1270.

Han, R., Meng, L., Guerrero, J. M., and Vasquez, J. C. (2017). Distributed nonlinear control with event-triggered communication to achieve current-sharing and voltage regulation in dc microgrids. *IEEE Transactions on Power Electronics*, 33(7):6416–6433.

Incremona, G. P., Cucuzzella, M., and Ferrara, A. (2016). Adaptive suboptimal second-order sliding mode control for microgrids. *International Journal of Control*, 89(9):1849–1867.

ISGF (2019). Distributed generation. http://www.indiasmartgrid.org/Distributed-Generation.php.

Jerin, A. R. A., Prabaharan, N., Kumar, N. M., Palanisamy, K., Umashankar, S., and Siano, P. (2018). 10 - smart grid and power quality issues. In Fathima, A. H., Prabaharan, N., Palanisamy, K., Kalam, A., Mekhilef, S., and Justo, J. J., editors, *Hybrid-Renewable Energy Systems in Microgrids*, Woodhead Publishing Series in Energy, pages 195 – 202. Woodhead Publishing.

Justo, J. J., Mwasilu, F., Lee, J., and Jung, J.-W. (2013). Ac-microgrids versus dc-microgrids with distributed energy resources: A review. *Renewable and sustainable energy reviews*, 24:387–405.

Kosaraju, K. C., Cucuzzella, M., Scherpen, J., and Pasumarthy, R. (2018). Differentiation and passivity for control of brayton-moser systems. *arXiv preprint arXiv:1811.02838*.

Lasseter, R. H. and Piagi, P. (2004). Microgrid: A conceptual solution. In *IEEE Power Electronics Specialists Conference*, volume 6, pages 4285–4291. Citeseer.

Leonard, J. P. (2014). Nonlinear modeling of dc constant power loads with frequency domain volterra kernels.

Lestas, I. (2019). Handout 2: Invariant sets and stability. http://www2.eng.cam.ac.uk/~icl20/4f3/Handout2.pdf.

Lotfi, H. and Khodaei, A. (2015). Ac versus dc microgrid planning. *IEEE Transactions on Smart Grid*, 8(1):296–304.

Mirakhorli, A. and Dong, B. (2016). Occupancy behavior based model predictive control for building indoor climate—a critical review. *Energy and Buildings*, 129:499–513.

Nasirian, V., Moayedi, S., Davoudi, A., and Lewis, F. L. (2014). Distributed cooperative control of dc microgrids. *IEEE Transactions on Power Electronics*, 30(4):2288–2303.

Nguyen, T.-L., Guillo-Sansano, E., Syed, M. H., Nguyen, V.-H., Blair, S. M., Reguera, L., Tran, Q.-T., Caire, R., Burt, G. M., Gavriluta, C., et al. (2018). Multi-agent system with plug and play feature for distributed secondary control in microgrid—controller and power hardware-in-the-loop implementation. *Energies*, 11(12):3253.

O'gorman, R. and Redfern, M. (2004). Voltage control problems on modern distribution systems. In *IEEE Power Engineering Society General Meeting, 2004.*, pages 662–667. IEEE.

Olivares, D. E., Mehrizi-Sani, A., Etemadi, A. H., Cañizares, C. A., Iravani, R., Kazerani, M., Hajimiragha, A. H., Gomis-Bellmunt, O., Saeedifard, M., Palma-Behnke, R., et al. (2014). Trends in microgrid control. *IEEE Transactions on smart grid*, 5(4):1905–1919.

Papathanassiou, S., Hatziargyriou, N., Strunz, K., et al. (2005). A benchmark low voltage microgrid network. In *Proceedings of the CIGRE symposium: power systems with dispersed generation*, pages 1–8. CIGRE.

Perez, F. and Damm, G. (2019). Dc microgrids. In *Microgrids Design and Implementation*, pages 447–475. Springer.

Rahmani, S., Saeidi, M., and Pirayesh, A. (2017). A combinational power sharing strategy based on master-slave and droop methods for power-electronics-interfaced distributed generation units operating in a dc micro-grid. In *2017 IEEE International Conference on Smart Energy Grid Engineering (SEGE)*, pages 1–6. IEEE.

Rinaldi, G., Cucuzzella, M., and Ferrara, A. (2017). Third order sliding mode observer-based approach for distributed optimal load frequency control. *IEEE Control Systems Letters*, 1(2):215–220.

Sadabadi, M. S., Shafiee, Q., and Karimi, A. (2017). Plug-and-play robust voltage control of dc microgrids. *IEEE Transactions on Smart Grid*, 9(6):6886–6896.

Saleh, M., Esa, Y., and Mohamed, A. A. (2018). Communication-based control for dc microgrids. *IEEE Transactions on Smart Grid*, 10(2):2180–2195.

Setiawan, M. A., Abu-Siada, A., and Shahnia, F. (2016a). New technique for power sharing in dc microgrids. In *2016 IEEE 2nd Annual Southern Power Electronics Conference (SPEC)*, pages 1–5. IEEE.

Setiawan, M. A., Abu-Siada, A., and Shahnia, F. (2016b). Voltage regulation in dc microgrids with various circuit configurations. In *2016 IEEE 2nd Annual Southern Power Electronics Conference (SPEC)*, pages 1–6. IEEE.

Shivashankar, S., Mekhilef, S., Mokhlis, H., and Karimi, M. (2016). Mitigating methods of power fluctuation of photovoltaic (pv) sources–a review. *Renewable and Sustainable Energy Reviews*, 59:1170–1184.

Su, W., Wang, J., and Roh, J. (2013). Stochastic energy scheduling in microgrids with intermittent renewable energy resources. *IEEE Transactions on Smart grid*, 5(4):1876–1883.

Trip, S., Bürger, M., and De Persis, C. (2014). An internal model approach to frequency regulation in inverter-based microgrids with time-varying voltages. In *53rd IEEE Conference on Decision and Control*, pages 223–228. IEEE.

Trip, S., Cucuzzella, M., Cheng, X., and Scherpen, J. (2018). Distributed averaging control for voltage regulation and current sharing in dc microgrids. *IEEE Control Systems Letters*, 3(1):174–179.

Trip, S., Cucuzzella, M., De Persis, C., Ferrara, A., and Scherpen, J. M. (2020). Robust load frequency control of nonlinear power networks. *International Journal of Control*, 93(2):346–359.

Tucci, M., Meng, L., Guerrero, J. M., and Ferrari-Trecate, G. (2018). Stable current sharing and voltage balancing in dc microgrids: A consensus-based secondary control layer. *Automatica*, 95:1–13.

Venkatraman, R. and Khaitan, S. K. (2015). A survey of techniques for designing and managing microgrids. In *2015 IEEE Power & Energy Society General Meeting*, pages 1–5. IEEE.

Wang, Z., Liu, F., Chen, Y., Low, S. H., and Mei, S. (2017). Unified distributed control of stand-alone dc microgrids. *IEEE Transactions on Smart Grid*, 10(1):1013–1024.

Weitenberg, E. (2018). Control of electrical networks: robustness and power sharing.

Zhao, J. and Dörfler, F. (2015). Distributed control and optimization in dc microgrids. *Automatica*, 61:18–26.

Appendix A

Benchmark network

A.1 Benchmark LV microgrid network

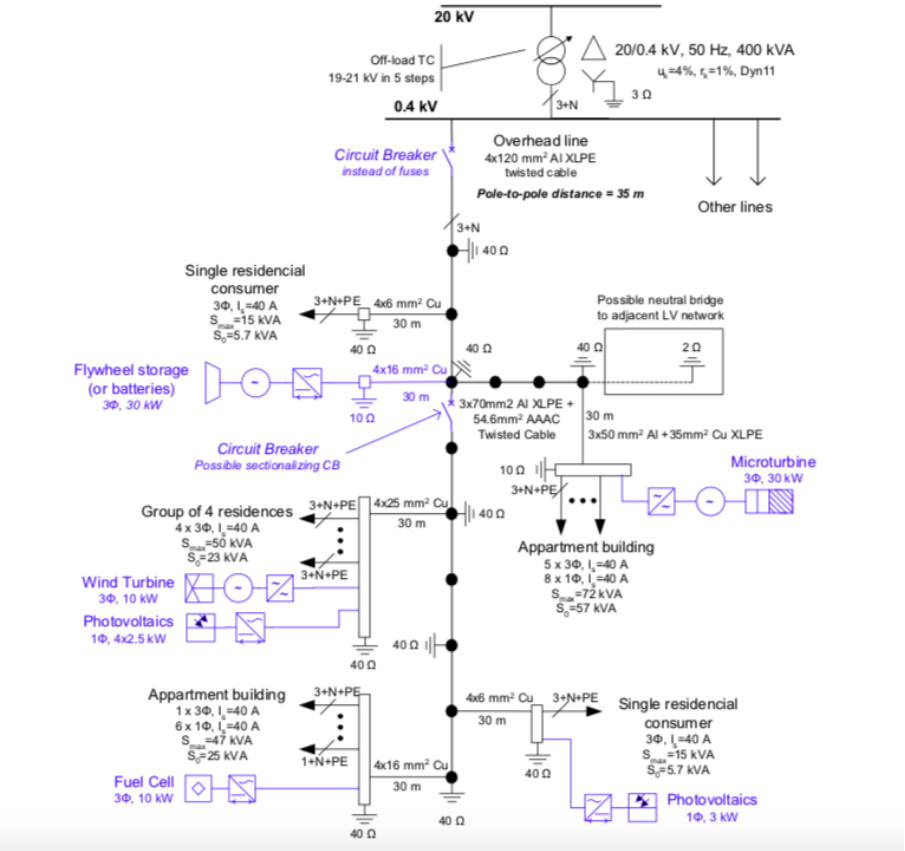

Figure A.1: Benchmark LV microgrid network (Papathanassiou et al., 2005)

A.2 Reduced benchmark LV microgrid network

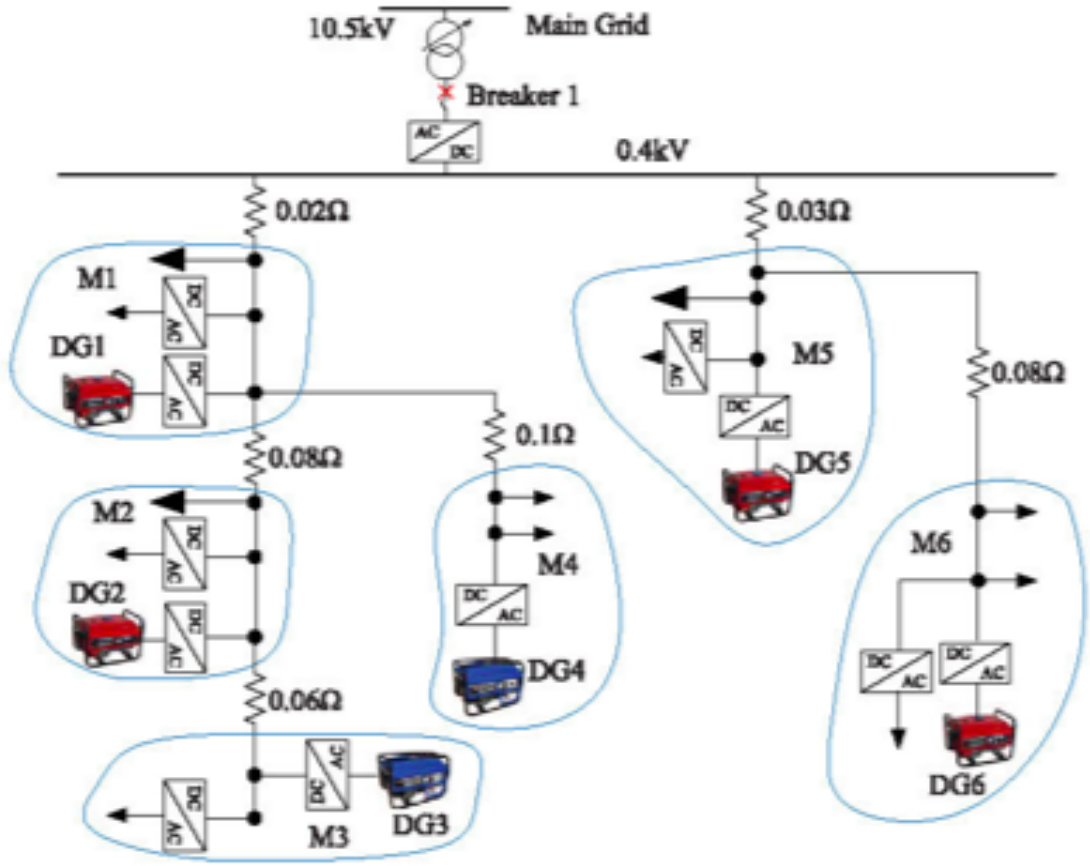

Fig. 2. Six-microgrid system.

Figure A.2: Reduced benchmark LV microgrid network (Wang et al., 2017)